The 2006 Eruption of Augustine Volcano, Alaska
Power, J.A., Coombs, M.L., and Freymueller, J.T., editors
U.S. Geological Survey Professional Paper 1769

Chapter 9

Timing, Distribution, and Character of Tephra Fall from the 2005–2006 Eruption of Augustine Volcano

By Kristi L. Wallace[1], Christina A. Neal[1], and Robert G. McGimsey[1]

Abstract

The 2005–6 eruption of Augustine Volcano produced tephra-fall deposits during each of four eruptive phases. Late in the precursory phase (December 2005), small phreatic explosions produced small-volume, localized, mostly nonjuvenile tephra. The greatest volume of tephra was produced during the explosive phase (January 11–28, 2006) when 13 discrete Vulcanian explosions generated ash plumes between 4 and 14 km above mean sea level (asl). A succession of juvenile tephra with compositions from low-silica to high-silica andesite is consistent with the eruption of two distinct magmas, represented also by a low-silica andesite lava dome (January 13–16) followed by a high-silica andesite lave dome (January 17–27). On-island deposits of lapilli to coarse ash originated from discrete vent explosions, whereas fine-grained, massive deposits were elutriated from pyroclastic flows and rock falls. During the continuous phase (January 28–February 10, 2006), steady growth and subsequent collapses of a high-silica andesite lava dome caused continuous low-level ash emissions and resulting fine elutriate ash deposits. The emplacement of a summit lava dome and lava flows of low-silica andesite during the effusive phase (March 3–16, 2006) resulted in localized, fine-grained elutriated ash deposits from small block-and-ash flows off the steep-sided lava flows.

Mixing of two end-member magmas (low-silica and high-silica andesite) is evidenced by the overall similarities between tephra-fall and contemporaneous lava-dome and flow lithologies and by the chemical heterogeneity of matrix glass compositions of coarse lapilli and glass shards in the ash-size fraction throughout the 2005–6 eruption. A total mass of 2.2×10^{10} kg of tephra fell (bulk volume of 2.2×10^{7} m^3 and DRE volume of 8.5×10^{6} m^3) during the explosive phase, as calculated by extrapolation of mass data from a single Vulcanian blast on January 17. Total tephra-fall volume for the 2005–6 eruption is about an order of magnitude smaller than other historical eruptions from Augustine Volcano. Ash plumes of short duration and small volume caused no more than minor amounts (≤1 mm) of ash to fall on villages and towns in the lower Cook Inlet region, and thus little hazard was posed to local communities. The bulk of the ash fell into Cook Inlet. Monitoring by the Alaska Volcano Observatory during the eruption helped to prevent hazardous encounters of ash and aircraft.

Introduction

Augustine Volcano, in the eastern Aleutian arc, has erupted seven times since 1812 and is the most historically active volcano in south-central Alaska's Cook Inlet region (Miller and others, 1998; fig. 1). The most recent eruption in 2005–6 produced ash clouds and fall, pyroclastic flows, and lava domes and flows, similarly to recent eruptions in 1986 and 1976. Four distinct eruptive phases, defined on the basis of the various processes that occurred during the eruption, each generated some form of tephra-fall deposit during this most recent eruption. The four phases include the (1) precursory (April–December 2005), (2) explosive (January 11–28, 2006), (3) continuous (January 28–February 10, 2006), and (4) effusive (March 3–16, 2006) phases (Power and others, 2006). Documentation of tephra fall was challenging because the volcano is on a remote island and most of the tephra fell on water. The eruption occurred during the winter, so tephra deposits on land were subject to high winds and fallout on ephemeral snow. Because tephra volumes were small, tephra that fell onto nearby land surfaces (25–185 km away) comprised fine ash dustings that were mostly less than 1 mm thick and posed little hazard to local populations. Proximal deposits are complex and varied because of near-vent processes, including elutriation from pyroclastic flows and rockfalls and

[1]Alaska Volcano Observatory, U.S. Geological Survey, 4200 University Drive, Anchorage, AK 99508.

modification by reworking. Calculations of tephra-fall volume are based on mass data for an ash-fall deposit from a discrete plume on January 17, 2006. This was the only opportunity to accurately determine tephra-fall volume for a single event, because it was deposited on land and was quickly buried by snowfall, and thus we formulate total mass and volume for all fall deposits erupted during the explosive phase by extrapolation of these data.

This report describes the timing, distribution, character, mass, and origin of tephra-fall deposits from the 2005–6 eruption of Augustine and concludes with a discussion of their significance and hazards. Because most of the explosive events were not observed directly, we infer their origins from time-lapse photography, geophysical data, and deposit characteristics. Magmatic or hydrovolcanic explosions at the vent initiated some tephra falls, and dome collapses that formed pyroclastic flows or rockfalls, and generated fine-grained elutriate ash clouds initiated others. Regardless of origin, tephra plumes resulted from these events and at times extended hundreds of kilometers downwind.

Methods

We describe tephra-fall deposits in terms of (1) time of eruption, (2) distribution, (3) character, including thickness, particle size, composition (componentry and glass geochemistry), and preservation, (4) origin, and (5) mass, when known. Samples collected for this study are archived at the U.S. Geological Survey (USGS) Alaska Tephra Laboratory and Data Center at the Alaska Volcano Observatory (AVO) in Anchorage, Alaska.

Timing of Tephra Production

We adopt the sequence and naming of eruption phases of Power and others (2006) to describe the timing of the 2005–6 eruption. We use event numbers to reference individual explosions of the explosive phase (Vallance and others, this volume; Power and others, 2006; table1).

Tephra Distribution

Explosions that generated discrete plumes had distinct seismic signals (Power and Lalla, this volume; McNutt and others, this volume) that alerted AVO to collect plume data and tephra samples. Data collected include (1) estimation of plume height (from radar and/or pilot reports; Schneider and others, 2006), (2) seismic duration of explosive event (Power and Lalla, this volume), (3) direction of prevailing winds, (4) movement direction of plume in satellite and radar data (Bailey and others, this volume; Schneider and others, 2006), (5) ash-fall reports from nearby towns and villages, and (6) overflight photography. Timely access to these data facilitated tracking of individual plumes. During the continuous phase, secondary plumes of elutriated fine ash from pyroclastic flows and rockfalls were more complicated to track because their onset times and plume heights were difficult to constrain. Tephra fall into Cook Inlet could not be documented, so deposits too small to reach adjacent landmasses 25 km away are not reported here. Herein, the term "proximal" implies Augustine Island and "distal" implies any landmass off the island (that is, Alaska mainland, Kenai Peninsula, Kodiak Island).

Available satellite images and radar data allow reconstruction of plume trajectories (fig. 1) at the time of plume generation and transport, and they closely match the wind forecast data from the National Weather Service (NWS) and the National Atmospheric and Oceanic Administration (NOAA) (fig. 2). Our telephone network allowed people in towns and villages along the path of drifting plumes to report observations of ash clouds and tephra fall, although much of the tephra fall occurred in sparsely settled or uninhabited areas. Other papers in this volume present more detailed data on plume trajectories and distribution using various satellite data (Bailey and others, this volume; Webley and others, this volume). With one exception, we did not reconstruct deposit isopachs, because tephra fell over water or in remote, uninhabited areas and because some tephra lobes overlapped to form a single undifferentiated layer. Plume heights in text are all from radar data (Schneider and other, 2006, and data taken from poster by D.J. Schneider and others, 2006) for consistency and differ from pilot-reported heights, although both are shown in table 1.

Tephra Character

We characterize tephra-fall deposits in terms of thicknesses when known, particle size, composition (componentry and glass geochemistry), and preservation. We collected proximal tephra samples at 65 field stations in July–August 2006 and during brief visits to the island and affected regions while the eruption was in progress (fig. 3 and appendix 1). We deployed ash-collection buckets on Augustine in late December 2005 in an attempt to collect temporally constrained samples during times when it was unsafe to be on the island. The buckets were colocated with geophysical instruments to facilitate recovery during brief visits to the island throughout the eruption. Distal samples were collected during the eruption either during helicopter-based fieldwork or by local citizens upon request.

We use standard volcanic terminology to characterize particle size (Fisher, 1961; Schmid, 1981; Chough and Sohn, 1990). We did not perform quantitative particle-size analyses because distal sample quantities were insufficient and, in proximal samples, deposits were reworked owing to wind or melting of underlying snow. We constructed generalized stratigraphic sections to represent proximal fall deposits on all four quadrants of the island to show the relations between deposits eruption (fig. 4). Sections are derived from best preserved

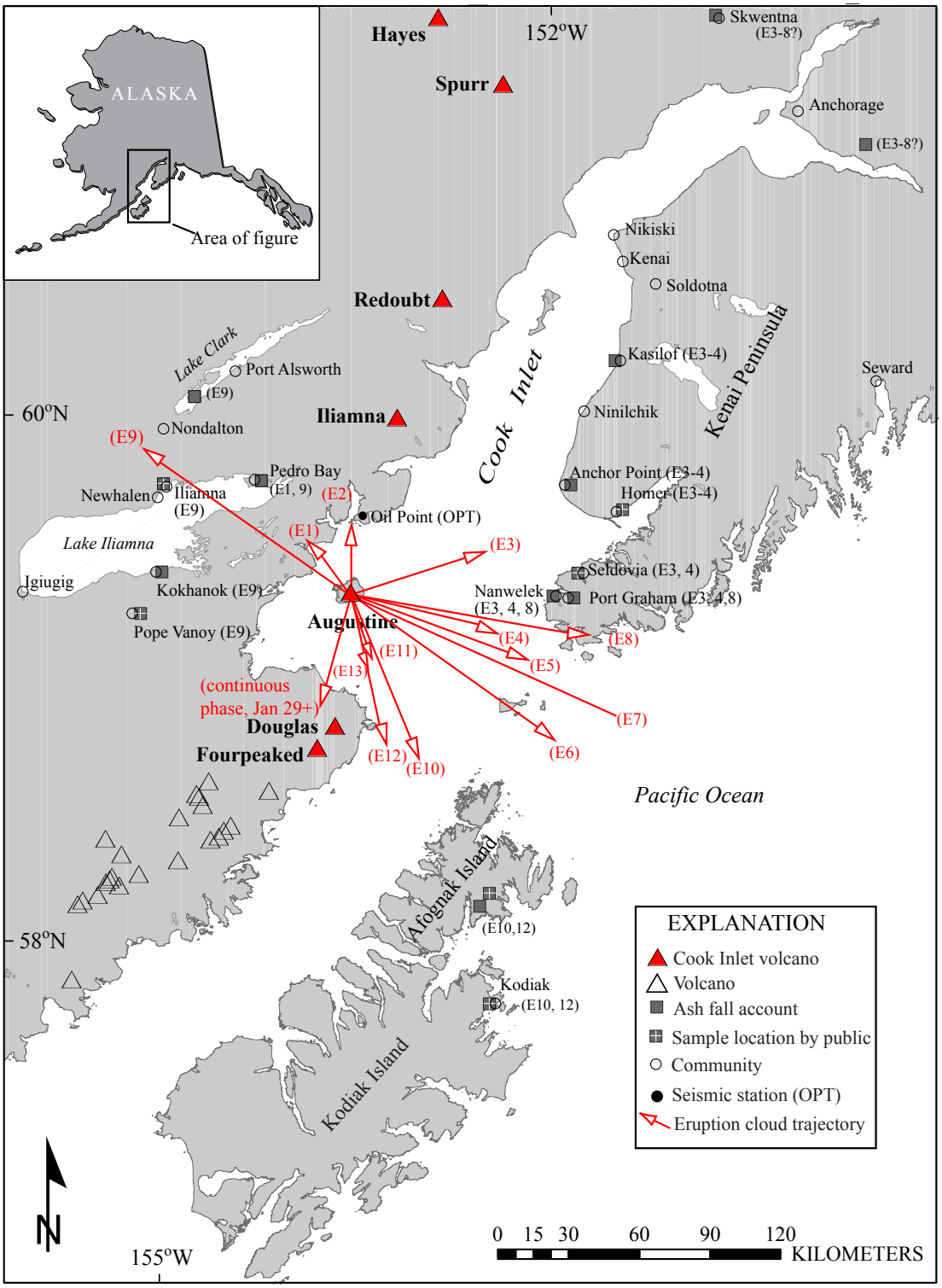

Figure 1. Map of south-central Alaska showing location of Augustine and other volcanoes, surrounding communities, ash-fall accounts, and ash-plume trajectories during the explosive and continuous phases of the 2005–6 eruption of Augustine. Plume trajectories are based on Nexrad radar data (data taken from poster of D.J. Schneider and others, 2006); E indicates explosive event number. Ash-fall accounts are eyewitness reports of ash fall. Such accounts are associated with event numbers but may fall off the path of the radar-derived plume trajectory, which indicates that shifting winds at different altitudes carried ash in those directions.

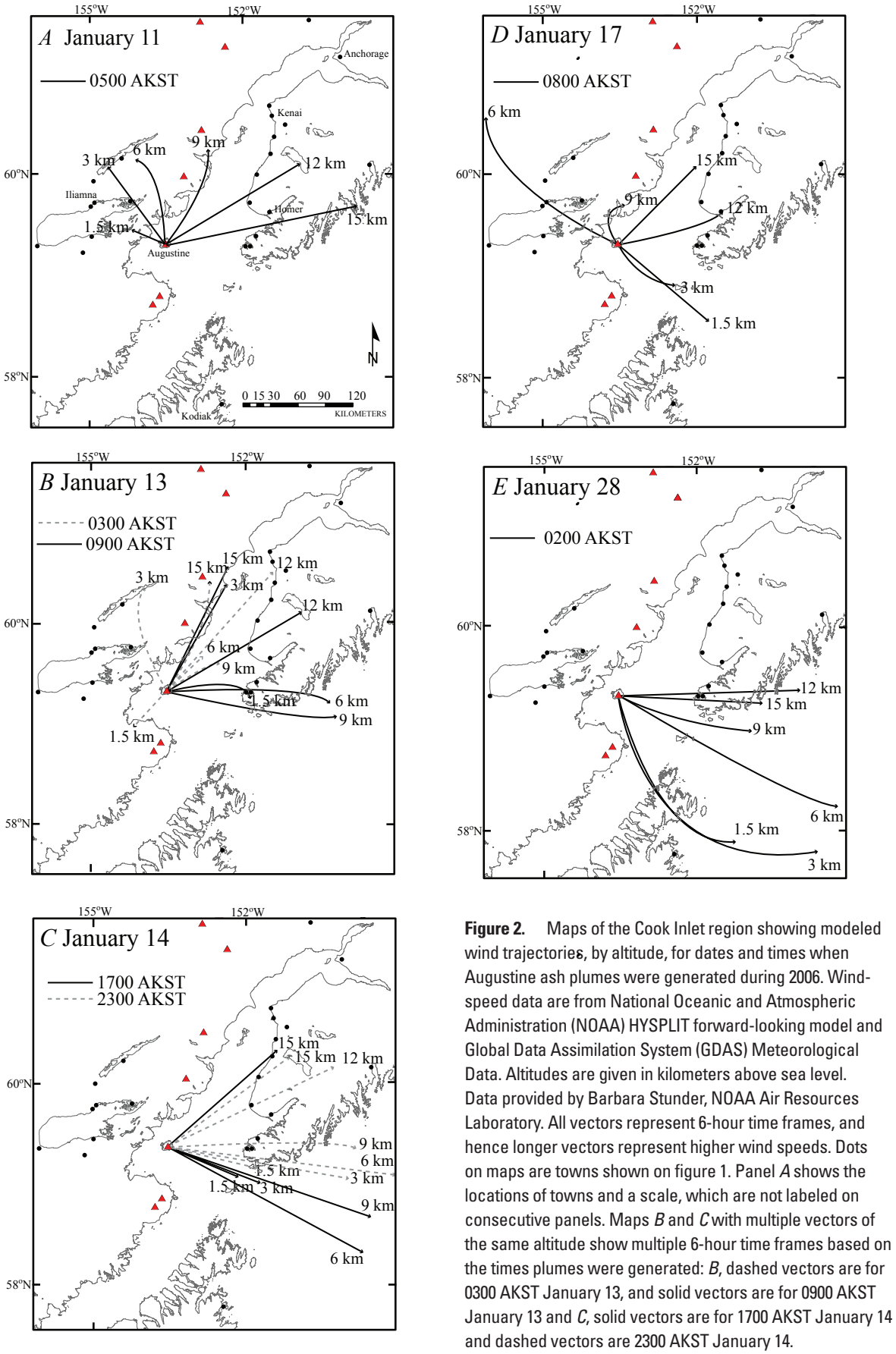

Figure 2. Maps of the Cook Inlet region showing modeled wind trajectories, by altitude, for dates and times when Augustine ash plumes were generated during 2006. Wind-speed data are from National Oceanic and Atmospheric Administration (NOAA) HYSPLIT forward-looking model and Global Data Assimilation System (GDAS) Meteorological Data. Altitudes are given in kilometers above sea level. Data provided by Barbara Stunder, NOAA Air Resources Laboratory. All vectors represent 6-hour time frames, and hence longer vectors represent higher wind speeds. Dots on maps are towns shown on figure 1. Panel *A* shows the locations of towns and a scale, which are not labeled on consecutive panels. Maps *B* and *C* with multiple vectors of the same altitude show multiple 6-hour time frames based on the times plumes were generated: *B*, dashed vectors are for 0300 AKST January 13, and solid vectors are for 0900 AKST January 13 and *C*, solid vectors are for 1700 AKST January 14 and dashed vectors are 2300 AKST January 14.

deposits protected by vegetation cover on the mid to lower flanks of the island.

Previous studies show that tephra from historical eruptions of Augustine have a range of glass compositions (for example, Kienle and Swanson, 1987; Johnston, 1978; Daley, 1986; and Roman and others, 2005). Therefore where possible, we use grain-discrete analysis of the glass fraction to help characterize the geochemistry of tephra deposits. Glass analyses were determined using a Cameca SX-50 electron microprobe at the University of Alaska Fairbanks Advanced Instrumentation Lab (table 2 and appendix 2). Analyses are of distal glass shards and of matrix glass of proximal lapilli. Brown, clear, and hybrid glass (mixture of brown and clear glass) identified throughout the eruption (fig. 5) posed some analytical challenges. Brown glass contains abundant microlites, while clear glass is mostly microlite free. Identifying pure glass pools in brown "glass" was challenging, and these data show significant scatter as a result. All glass analyses were filtered to eliminate the inclusion of mineral data (appendix 2), although the distinction between truly heterogeneous glass and scatter resulting from partial analysis of glass plus microlites is sometimes difficult to make. Larsen and others (this volume, their table 4) show glass analyses from tephra-fall deposits where they made a concerted effort to identify pure glass pools using backscatter imaging on the electron microprobe. For brevity, we pared down the hundreds of glass analyses that we performed to a summary of ranges of compositions listed by eruptive phase, event number, and lithology (table 2). Raw, filtered glass compositions are given in appendix 2.

We did component analyses using proximal, coarse-grained deposits and sorted clasts > 5mm into lithologies based on macroscopic appearance (table 3, fig. 5). The resulting lithologic types are the same as those used by researchers studying other proximal products from the eruption (Coombs and others, this volume; Vallance and others, this volume; Larsen and others, this volume). Component analyses are reported in percent of n clasts per sample.

Preservation of both distal and proximal tephra-fall deposits is discussed, because we think it is an important consideration for the future interpretation of these deposits as well as for the understanding of prehistoric tephra records, at least in this region. Eruption histories deciphered using Holocene tephrostratigraphic studies often show only minimum numbers of eruptions, because tephra-fall deposits are not always faithfully recorded in the geologic record (for example, Riehle, 1985; de Fontaine and others, 2007; Schiff and others, 2008). Thus, a discussion of preservation (or lack of) here is relevant to interpreting prehistoric tephra-fall records when direct observations were not made.

Tephra Origin

Multiple volcanic processes can generate ash clouds and ash fall—short-lived blasts, either magmatic or phreatic; sustained magmatic eruption; and elutriation of ash from pyroclastic flows. Integration of field observations and laboratory analyses of tephra-fall and other deposits of the 2005–6 eruption of Augustine is critical to interpreting the origins of the fall deposits. Close coordination with researchers who studied other aspects of the eruption (Coombs and others, this volume; Vallance and others, this volume; Larsen and others, this volume) allowed for consistent identification and characterization of all eruptive products. Evidence used to interpret deposit origin includes (1) duration of plume generation and plume height, (2) volume of fall deposits, (3) componentry of fragmental deposits, (4) contemporaneous volcanic activity, (5) seismicity, (6) acoustic signals, and (7) gas and steam emissions.

Tephra Mass

We used mass-per-unit-area sampling to calculate mass and volume of tephra fall. The mass per unit area (g/m^2) of a sample is the mass (g) of dried sample divided by the area (m^2) from which the sample was collected. These values were plotted on a base map, and contours of equal mass (isomass contours) were constructed. On the basis of our coarse sampling, we were able to draw four isomass contours: 10, 50, 100, and 10,000 g/m^2. Total mass of the tephra deposit was then calculated using the root-area method developed by Pyle (1989) and modified by Fierstein and Nathenson (1992) (table 4). This method accounts for the mass of tephra that fell beyond the most distal isomass contour (that is, 0 g/m^2). We calculate bulk and dense-rock-equivalent (DRE) deposit volume by assuming a bulk density of 1,000 kg/m^3 and a rock density of 2,600 kg/m^3, then dividing the total mass by these densities (Sarna-Wojcicki and others, 1981) (table 4). When calculating eruption rates (erupted mass/eruption duration), we use seismic duration at a distant station (32 km from Augustine; Power and Lalla, this volume) as a proxy for the length of time that a plume was generated (fig. 1).

We used mass per unit area, rather than deposit thickness, to calculate tephra-fall mass and volume, because individual deposits fell in place along with snow and subsequently were buried by snowfall. Modification by compaction does not alter results using this method (Scott and McGimsey, 1994). Tephra was collected from 10 sites of areas 0.04 to 0.25 m^2 (20×20 cm to 50×50 cm), depending on the amount of ash present. The tephra was preserved as a layer in the snowpack, which facilitated sampling the thin and sometimes diffuse deposit (fig. 6). Several snow pits were excavated at each sample site to expose the deposit and to select a representative sample location. Snow overlying the tephra deposit was shoveled away, a plastic measured-area template was placed on the deposit, and a trowel was used to trace out the measured area. The tephra deposit and some underlying snow were collected into large plastic, sealable bags using a trowel. In addition to tephra from the snowpack, one sample was collected on January 17 by a resident of the village of Iliamna, 90 km northwest of Augustine, who collected falling ash on a measured piece of aluminum foil.

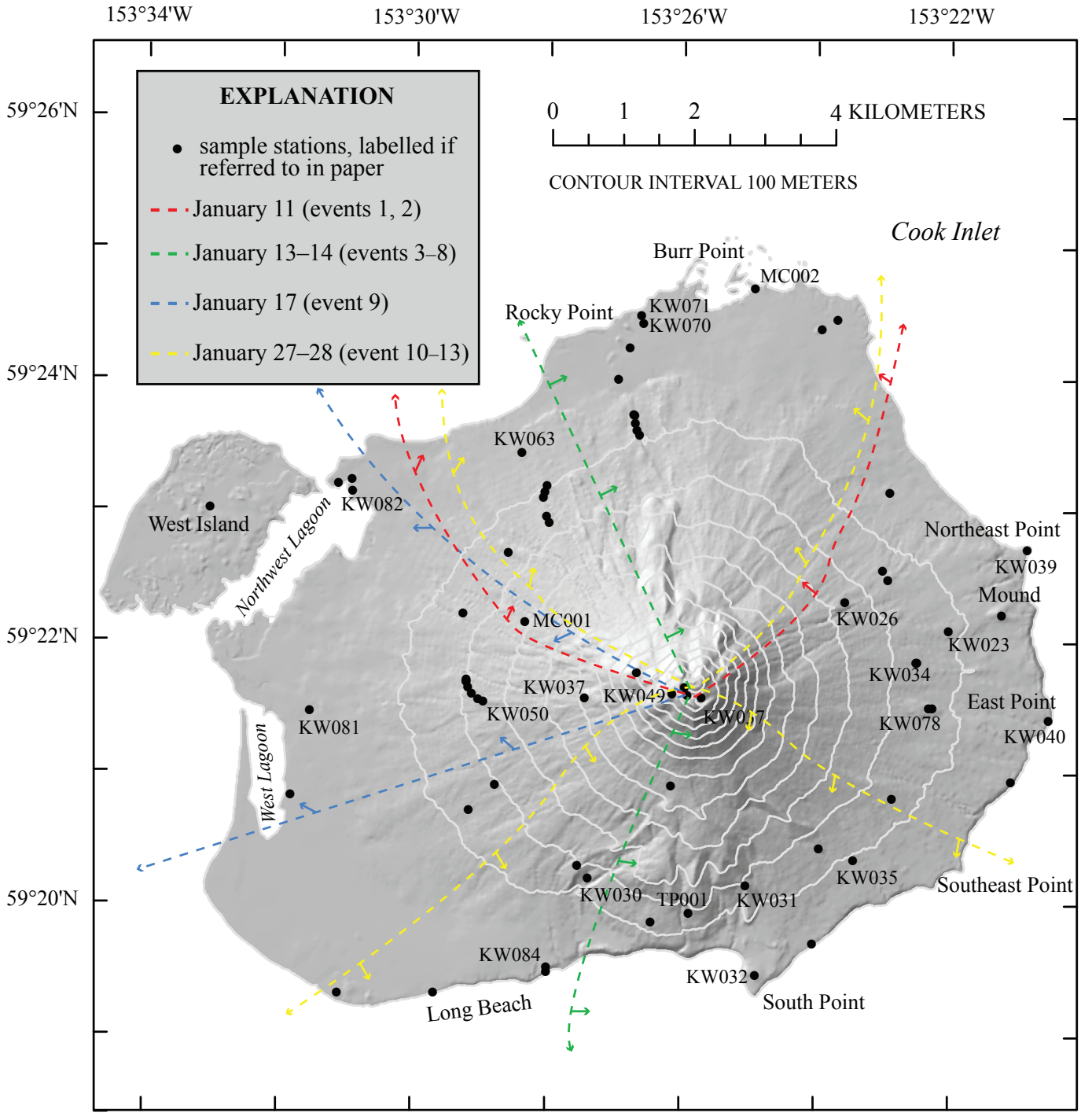

Figure 3. Shaded relief map of Augustine Island showing sample locations (black dots) for this study and dashed lines indicating the boundaries of ash-fall deposits from explosive events that occurred during the explosive phase of the 2005–6 eruption (January 11–28, 2006). Station names are shown for all samples referred to in the paper. Common geographic place names are shown though all except Burr Point are informal. Digital elevation model from 1990.

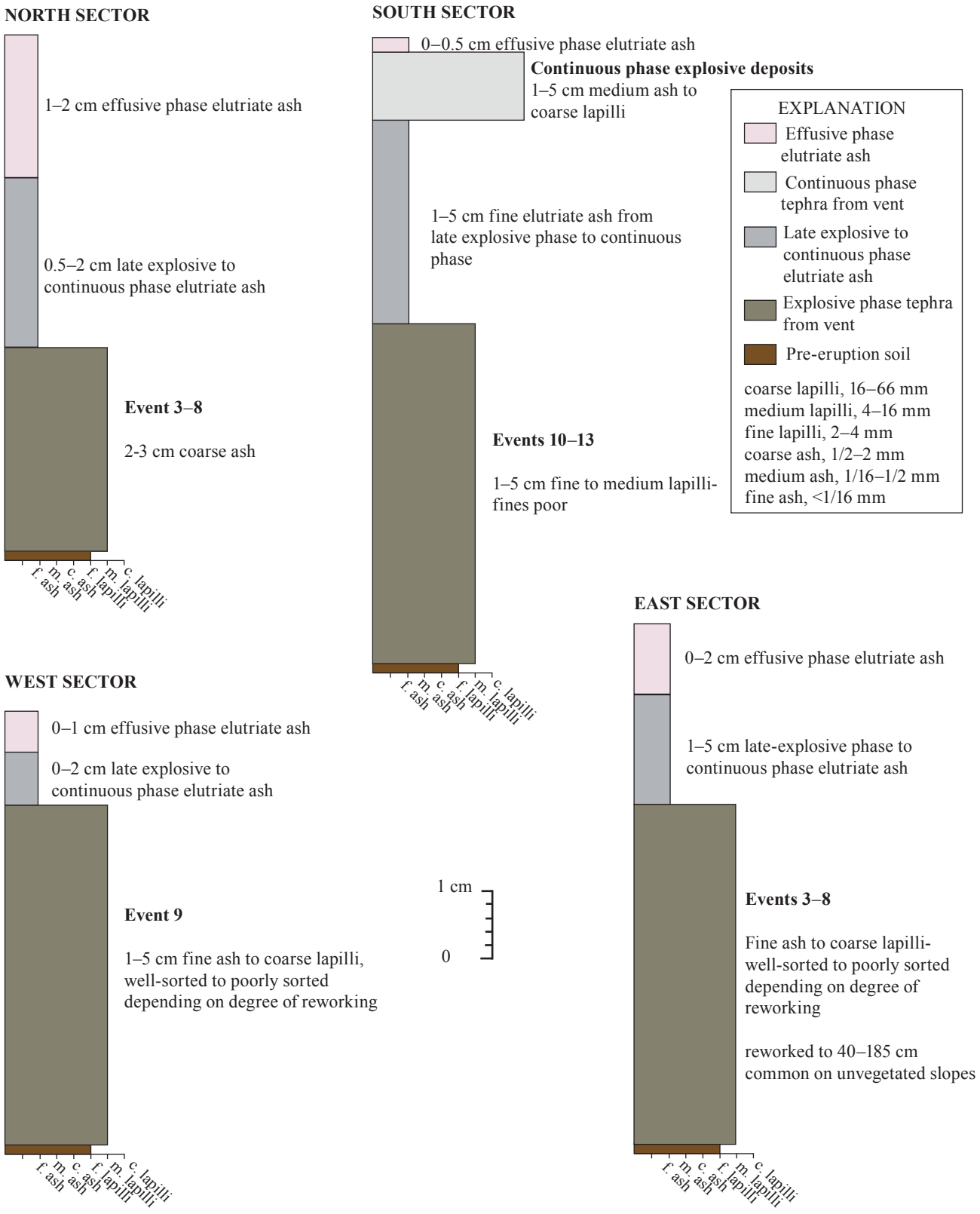

Figure 4. Generalized stratigraphic sections by volcano sectors, showing relations between and characteristics of proximal tephra-fall deposits from the explosive, continuous, and effusive phases of the 2005–6 eruption. Sections are derived from best preserved deposits in vegetated areas on the mid to lower slopes of the island.

Distribution, Character, and Origin of Tephra Deposits

In the following section, we describe in chronological order the tephra-fall deposits that formed during the four discrete phases of the 2005–6 eruption. For each phase, we describe the main eruptive phenomena, describe the resulting tephra deposits, and discuss the origin of tephra generated.

Precursory Phase Tephra Deposits (December 2005)

Distribution and Character of Precursory Phase Tephra

Following more than 7 months of increasing volcanic unrest in the form of seismicity and edifice inflation (Cervelli and others, this volume), several seismic signals suggested a series of small volcanic explosions at Augustine in mid-December. The three largest occurred on December 10, 12, and 15 (Power and others, 2006; Power and Lalla, this volume). Visual observations, radar, and satellite imagery failed to detect the ash plumes from these explosions because they were small or contained very little ash. Nonetheless, we were able to document resulting deposits during observation overflights and landings on the island within days of their occurrence.

A discontinuous, dark-colored dusting of fine to medium ash was observed on the island on December 12. This minor tephra-fall deposit was restricted to the southern sector of Augustine Island and nearby Cook Inlet. A sample collected on December 20 comprises both altered and fresh-looking, possibly juvenile, glass shards (fig. 3, sample TP001). The bulk of the deposit is fragments of altered rock and crystal fragments that are likely reworked older volcanic material.

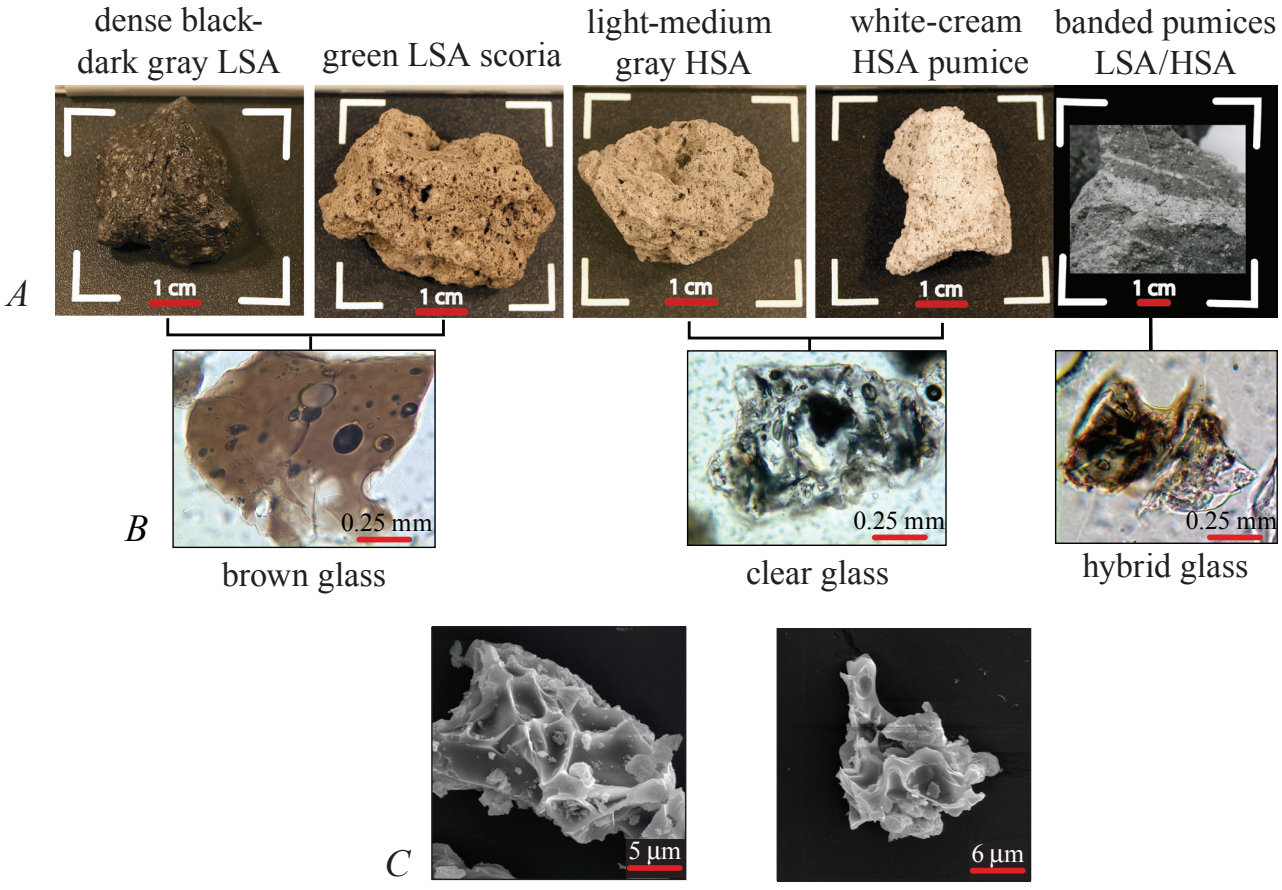

Figure 5. Photographs, photomicrographs, and SEM image of Augustine tephra. *A*, Photographs illustrating clast types erupted during the explosive phase, January 11–28, 2006. LSA, low silica andesite; HSA, high silica andesite. *B*, Transmitted-light photomicrographs illustrating glass phases, including brown, clear, and hybrid varieties. Typically, clear glass is associated with HSA magma and brown glass is associated with LSA magma, although most clasts contain a mixture of both magma compositions. *C*, Scanning electron microscope (SEM) image of vesicular ash particles erupted by Augustine Volcano on January 13, 2006. SEM photographs courtesy of Pavel Izbekov, University of Alaska Fairbanks.

Unaltered glass shards and pumice composed of both clear and brown glass show a range of SiO_2 between 73 and 77.5 wt. percent (table 2 and fig. 7). Reworking by high winds, deposition on snow cover and subsequent burial by younger tephra-fall deposits have now obliterated this deposit as a distinct entity from the geologic record.

Origin of Precursory Phase Tephra

Plumes that are not radar-reflective, the very small volume of deposits, and a lack of clear evidence of juvenile material, coupled with the presence of altered and clearly older lithic fragments, lead us to interpret these tephra deposits as being the result of phreatic explosions. Further evidence, such as impulsive, shallow seismicity suggestive of hydrothermal activity and a marked increase in gas and steam emissions above background levels at the volcano support this interpretation (Power and Lalla, this volume; Buurman and West, this volume; McGee and others, this volume).

Explosive Phase Tephra Deposits (January 11–28, 2006)

Distribution and Character of Explosive Phase Tephra

From January 11–28, a total of 13 discrete explosions sent ash plumes between 4 and 14 km asl and produced tephra fall downwind along several azimuths from the volcano (table 1, fig. 1). Strong seismicity associated with these events lasted 1–11 minutes (averaging 4 minutes; Power and Lalla, this volume) and closely matched the duration of plume generation. Plumes quickly detached from the vent and were distributed downwind (Bailey and others, this volume). The discrete and brief character of these explosions allowed us to discriminate individual ash clouds and to track their distribution using Nexrad radar (Schneider and others, 2006), satellite-image analysis (Bailey and others, this volume), and eyewitness reports. On January 11, 13, and 14, several plumes were generated within hours of one another (table 1) and subsequently coalesced. In such cases, individual ash clouds are poorly differentiated (Bailey and others, this volume). Minor amounts of tephra (1–3 mm) commonly fell between 25 and 185 km downwind from the volcano, and trace amounts (<0.5 mm) of fine ash were reported on one occasion as far as Castella, California, nearly 3,000 km southeast of Augustine.

Figure 6. Photograph showing measured-area sampling of an Augustine ash deposit (from January 17, 2006) preserved in the snow pack west of the volcano near Lake Iliamna. Photo by Christina Neal, March 10, 2006.

January 11, 2006 (Explosive Events 1 and 2)

Two explosions within 30 minutes, events 1 and 2, generated ash plumes to maximum heights of 6.5 and 10.2 km asl, respectively (Schneider and others, 2006). Radar data and satellite images show that the first of the two plumes traveled northwest, and ash fall was reported from villages surrounding Lake Iliamna, 25–80 km west and northwest of Augustine (fig. 1). Satellite images showed that the second ash plume traveled northeast over Cook Inlet, and no deposits were preserved.

On January 12, a field crew visited Augustine Island, and oblique aerial photographs taken that day show a dark-colored, distinct tephra deposit on the south flank and a less obvious dusting of ash on the snow-covered west and north flanks. Low-level ash emissions observed that day probably formed the dark spokelike fall deposit on the south, but we infer the ash on the west and north to have formed during events 1 and 2 (fig. 3). Observations suggested that the preexisting dome complex was partially destroyed during this explosion (Coombs and others, this volume). No tephra-deposit thicknesses were recorded. Samples collected from the west and north flanks of the volcano consist of coarse ash to lapilli with coatings of fine ash (table 3 and fig. 3, samples MC001 and MC002). The coarse fraction includes mainly gray, angular-to-subrounded, dense glassy-to-crystalline fragments and free crystal fragments. Orange, yellow, and red altered clasts of dense lava fragments are common. Vesicular particles are rare. We cannot determine whether the fresh-looking dense fragments are juvenile or recycled tephra or lava from previous eruptions.

A distal tephra-fall deposit, presumably from event 1, was sampled on March 10, 2006, 30 km northwest of Augustine. The deposit was dark colored and present as either a discrete 1–3 mm thick layer or distributed over a depth of 5 mm in the snow pack and underlying a fall deposit from event 9 (January 17) in this region (fig. 8). The event 1 deposit ranges from fine to coarse ash and contains a mixture of old-looking crystallized particles and fresh-looking unaltered clear, brown, and

Table 1. Summary of significant tephra-producing events of the 2005–2006 eruption of Augustine Volcano.

[Duration of seismic signal at station OPT is used as a proxy for duration of plume generation (Power and Lalla, this volume). Plume heights determined from Nexrad radar (data from poster of D.J. Schneider and others, 2006) and have error of ± 1.5 km (D.J. Schneider, oral commun., 2006); plume heights from pilot reports (PIREPs) are from the National Weather Service or Federal Aviation Administration. Plume direction based on satellite data (Bailey and others, this volume), National Oceanic and Atmospheric Administration HYSPLIT model forward trajectories, GDAS meteorological data, and eyewitness accounts. Maximum distance of tephra fall was from confirmed eyewitness reports or from Moderate Resolution Imaging Spectroradiometer (MODIS) satellite imagery. Observation of event: PIREP, pilot report; ph, overflight and fieldwork photograph; st, satellite images; web, web camera; tl, time-lapse camera; dep, photographs of deposits. Origin of tephra plume: vp, ash plume originating from vent; pf, ash cloud from elutriation of pyroclastic flow; rf, ash cloud from a rockfall event. Date of observation overflight for ease of identifying images in the Alaska Volcano Observatory image database (*http://www.avo.alaska.edu/images/*). nd, no data. All dates from 2006 unless noted.]

Event date, AKST (UTC)	Event no.	Event time, AKST	Seismic duration at OPT, min:sec	Plume height, in km asl	Plume height source	Plume direction	Maximum distance, in km	Observation of event	Origin of plume	Eye-witness account	Date of observation flight
					Precursory Phase						
12/15/05	nd	nd	nd	nd	nd	nd	nd	dep	vp	F	12/20/05
					Explosive phase						
1/11	1	4:44:00	01:18	6.5	radar	N, NE, NW	80	dep, st	vp	T	1/11, 1/12
1/11	2	5:12:00	03:18	10.2	radar	N, NW	80	dep, st	vp	T	1/11, 1/12
1/13	3	4:24:00	11:00	10.2	radar	E-SE	120	ph, st, dep	vp	T	1/16
1/13	4	8:47:00	04:17	10.2	Radar	E-SE	120	ph, st, dep, PIREP, web, tl	vp	T	1/16
				14-15	PIREP						
				16.0	PIREP						
1/13	5	11:22:00	03:24	10.5	radar	SE	120	ph, st, dep, PIREP, web, tl	vp	T	1/16
				16.0	PIREP						
1/13 *(01/14)*	6	16:40:00	04:00	10.5	radar	SE	120	ph, st, dep, PIREP, web, tl	vp	T	1/16
				9-11	PIREP						
1/13 *(01/14)*	7	18:58:00	03:00	13.5	radar	E SE	120	ph, st, dep	vp	T	1/16
1/14	8	0:14:00	03:00	10.2	radar	E SE	120	ph, st, dep	vp		1/16
1/17	9	7:58:00	04:11	13.5	Radar, PIREP	NW	140	ph, st, dep, PIREP	vp	T	1/18, 1/24
1/27 *(01/28)*	10	20:24:00	09:00	10.5	radar	SE	185	dep, st	vp	T	1/29, 1/30
1/27	11	23:37:21	01:02	3.8	radar	S SE	185	dep, st	vp	T	1/29, 1/30
1/28	12	2:04:13	02:06	7.2	radar	S SE	185	dep, st	vp	T	1/29, 1/30

1/28	13	7:42:00	03:00	7.2	radar	S SE	185	ph, st, dep, PIREP, web	vp	T	1/29, 1/30
Continuous phase											
1/28	14	14:31:00	nd	3.8	radar		185	ph, st, dep, PIREP, web	vp, pf	T	1/29, 1/30
				8.0	PIREP						
				9.0	PIREP						
1/29	nd	11:17:00	05:30	7.2	radar	S SW	185	ph, st, dep, PIREP, tl	vp, pf	T	1/29, 1/30
				9.0	PIREP						
				15.0	PIREPs						
1/30	nd	3:25:00	02:04	7.2	radar	NE	160	ph, st, dep, PIREP	vp, pf	T	1/30, 2/3, 2/8
				4.0	radar						
1/30	nd	6:21:00	nd	7.2	radar	E NE	160	ph, st, dep	vp, pf		1/30, 2/3, 2/8
2/8/07			nd	nd	nd	N - local	nd	ph, web	pf	F	2/8
Effusive phase											
3/4, 3/6, 3/7, 3/9, 3/10	nd	nd	nd	nd	nd	nd	85	ph, dep, web	rf, pf	T	3/6, 3/9, 3/10, 3/15

Table 2. Summary of groundmass glass average compositions for 2005–6 tephra from Augustine Volcano.

[All glass compositions determined using a Cameca SX-50 electron microprobe equipped with four wavelength-dispersive spectrometers and one energy-dispersive spectrometer at the University of Alaska Advanced Instrumentation Laboratory, Fairbanks, Alaska. Glasses analyzed using 15KeV, 10nA, and 10 micron-wide defocused beam. Oxide values given in weight percent and normalized to 100 percent anhydrous. Stdev, standard deviation; n, number of shards analyzed; GS, glass shard; MG, matrix glass from lapilli clast.]

Sample No.	SiO_2	TiO_2	Al_2O_3	FeO	MgO	CaO	Na_2O	K_2O	MnO	Cl	Total	Sample type
Precursory phase—December 2005												
clear glass-sample AT-703A.												GS
mean	76.96	0.26	13.30	1.46	0.28	2.07	3.85	1.71	nd	0.12	98.09	
stdev	0.62	0.33	0.90	0.76	0.22	0.68	1.23	0.85	nd	0.16		
n	7											
brown glass-sample AT-703B.												GS
mean	73.93	1.10	13.13	2.06	0.49	2.18	4.00	2.81	nd	0.27	97.69	
stdev	0.98	0.83	0.53	0.50	0.40	0.60	1.08	1.78	nd	0.09		
n	4											
Explosive phase—January 11, 2006, explosive events 1–2												
brown glass-samples AT-746, AT-769, AT-753, and AT-761.												GS
mean	65.56	0.96	16.44	4.22	1.68	4.78	4.68	1.54	nd	0.13	98.71	
stdev	0.89	0.32	0.48	0.52	0.61	0.70	0.33	0.23	nd	0.10		
n	5											
clear glass-samples AT-746, AT-769, and AT-761.												GS
Mean	77.09	0.23	12.38	1.57	0.22	1.84	4.51	2.01	nd	0.13	99.51	
stdev	0.88	0.17	0.38	0.37	0.10	0.67	0.32	1.18	nd	0.11		
n	9											
Explosive phase—January 13–14, 2006, explosive events 3–8												
dense low-silica andesite (DLSA)-samples AT-957B, AT-920A, and AT-967D.												MG
mean	68.16	0.84	15.27	3.55	0.80	4.10	5.01	2.00	0.05	0.23	99.81	
stdev	1.48	0.23	0.79	0.66	0.24	0.44	0.25	0.14	0.05	0.09		
n	11											
low-silica andesite scoria (LSAS)-samples AT-960A, AT920B, and AT-967A.												MG
mean	66.56	1.17	14.50	4.93	1.58	4.39	4.67	1.68	0.13	0.40	98.48	
stdev	1.02	0.16	0.57	1.04	0.27	0.36	0.39	0.10	0.05	0.13		
n	5											
high-silica andesite pumice (HSA)-sample AT-912D.												MG
mean	75.00	0.25	12.51	2.25	0.45	2.10	4.93	2.08	0.09	0.34	98.59	
stdev	0.53	0.13	0.45	0.71	0.04	0.11	0.32	0.06	0.03	0.13		
n	7											
Explosive phase —January 17, 2006, explosive event 9												
low-silica andesite scoria (LSAS)-samples AT-924A, AT-934A, AT905B, AT-943A, AT-949A.												MG
Mean	66.99	0.98	14.74	4.51	1.38	4.19	4.89	1.83	0.13	0.35	98.12	
stdev	1.59	0.20	1.10	0.63	0.22	1.13	0.39	0.49	0.10	0.12		
n	8											

Table 2. Summary of groundmass glass average compositions for 2005–2006 tephra from Augustine Volcano.—Continued

[All glass compositions determined using a Cameca SX-50 electron microprobe equipped with four wavelength-dispersive spectrometers and one energy-dispersive spectrometer at the University of Alaska Advanced Instrumentation Laboratory, Fairbanks, Alaska. Glasses analyzed using 15KeV, 10nA, and 10 micron-wide defocused beam. Oxide values given in weight percent and normalized to 100 percent anhydrous. Stdev, standard deviation; n, number of shards analyzed; GS, glass shard; MG, matrix glass from lapilli clasts.]

Sample No.	SiO_2	TiO_2	Al_2O_3	FeO	MgO	CaO	Na_2O	K_2O	MnO	Cl	Total	Sample type
Explosive phase—January 17, 2006, explosive event 9												
dense low-silica andesite (DLSA)-samples AT-940B , AT-923A, and AT-961B.												MG
mean	66.36	0.92	15.45	4.78	1.05	4.90	4.65	1.55	0.18	0.16	100.15	
stdev	1.21	0.16	1.01	0.71	0.23	0.55	0.24	0.20	0.09	0.06		
n	5											
high-silica andesite pumice (HSA)-samples AT-934B, AT-925C, AT-924C, and AT-961C.												MG
mean	74.42	0.47	12.34	2.36	0.41	2.10	5.23	2.25	0.07	0.34	100.38	
stdev	0.69	0.17	0.93	0.70	0.12	0.14	0.38	0.30	0.07	0.21		
n	6											
clear glass-samples AT-757, AT-759, AT-751, AT-744, AT-748, AT-767, AT-764, and AT-762.												GS
mean	76.25	0.47	12.36	1.89	0.33	1.45	4.03	3.07	nd	0.15	99.71	
stdev	0.91	0.38	0.71	0.34	0.20	0.75	0.62	1.48	nd	0.12		
n	13											
brown glass-samples AT-757, AT-759, AT-751, AT-744, AT-748, AT-767, and AT-762.												GS
mean	71.72	0.57	15.36	1.93	0.34	3.13	4.78	2.03	nd	0.15	99.12	
stdev	0.80	0.70	1.67	0.84	0.23	0.82	0.34	0.50	nd	0.15		
n	13											
Explosive phase —January 27–28, 2006, explosive events 10–13												
dense low-silica andesite (DLSA)-samples AT-932A, and AT-917A.												MG
mean	68.88	1.01	14.34	3.58	0.83	4.09	5.10	1.83	0.10	0.24	98.96	
stdev	4.00	0.66	0.81	2.61	0.89	0.58	0.06	0.18	0.14	0.17		
n	2											
high-silica andesite pumice (HSA)-sample AT-928A.												MG
mean	76.10	0.30	12.61	0.98	0.15	2.06	5.12	2.41	0.14	0.13	99.14	
stdev	0.20	0.02	0.66	0.42	0.01	0.09	0.35	0.19	0.10	0.11		
n	2											
clear glass-samples AT-733, AT-719, and AT-916.												GS
mean	75.30	0.26	13.29	1.11	0.31	1.93	4.98	2.61	0.06	0.18	100.04	
stdev	0.52	0.30	0.96	0.62	0.11	0.37	0.15	0.70	0.08	0.17		
n	3											
brown glass-sample AT-733.												GS
mean	69.28	0.60	15.88	2.79	0.85	4.09	4.52	1.72	0.03	0.24	98.80	
n	1											
Continuous phase—January 28–February 10												
clear glass-samples AT-770, AT-913, AT-909, and AT-953.												
Mean	76.04	0.50	12.52	1.63	0.32	1.76	4.60	2.35	0.12	0.21	99.68	GS

Table 2. Summary of groundmass glass average compositions for 2005–2006 tephra from Augustine Volcano.—Continued

[All glass compositions determined using a Cameca SX-50 electron microprobe equipped with four wavelength-dispersive spectrometers and one energy-dispersive spectrometer at the University of Alaska Advanced Instrumentation Laboratory, Fairbanks, Alaska. Glasses analyzed using 15KeV, 10nA, and 10 micron-wide defocused beam. Oxide values given in weight percent and normalized to 100 percent anhydrous. Stdev, standard deviation; n, number of shards analyzed; GS, glass shard; MG, matrix glass from lapilli clasts.]

Sample No.	SiO_2	TiO_2	Al_2O_3	FeO	MgO	CaO	Na_2O	K_2O	MnO	Cl	Total	Sample type
Continuous phase—January 28–February 10												
clear glass-samples AT-770, AT-913, AT-909, and AT-953.												
stdev	0.82	0.29	0.43	0.32	0.11	0.34	0.33	0.29	0.08	0.06		
n	21											
brown glass-samples AT-770, AT-909, and AT-953.												
mean	67.74	0.39	17.02	2.46	0.92	5.02	4.38	1.83	0.14	0.14	98.34	GS
stdev	1.72	0.36	1.51	0.95	0.41	1.19	0.82	0.81	0.02	0.17		
n	5											
Effusive phase—March 3–16												
clear glass-samples AT-915 and AT-919.												GS
mean	74.67	0.38	12.62	2.08	0.40	2.10	5.19	2.16	0.12	0.30	100.75	
stdev	0.36	0.07	0.09	0.19	0.07	0.13	0.21	0.10	0.05	0.08		
n	4											
brown glass-samples AT-915 and AT-919.												GS
mean	65.26	0.66	15.87	4.01	1.57	5.17	5.35	1.55	0.26	0.32	100.19	
stdev	0.94	0.04	0.08	0.50	0.82	0.47	0.53	0.19	0.10	0.16		
n	3											

hybrid glassy particles. Glass compositions range between 65–67 and 76–78 wt. percent silica (SiO_2) for brown and clear glass, respectively (table 2 and fig. 7).

Because of reworking by high winds, deposition onto snow, and subsequent burial by younger tephra-fall deposits, we recognized no primary exposures on the island following the eruption. Distal deposits are also not likely to be preserved in the geologic record owing to their small volume, deposition onto snowpack, and reworking by surface runoff.

January 13–14, 2006 (Explosive Events 3–8)

On January 13 and 14, six discrete explosions (events 3–8) produced ash plumes that reached between 10 and 13.5 km asl and that dispersed to the east-southeast (Schneider and others, 2006; fig. 1).

The Kenai Peninsula communities of Homer, Seldovia, Nanwelek, and Port Graham, 90–120 km downwind of Augustine, reported ash fall. In many cases ash fell with snow and snowflakes were particularly large and intricate, probably because of nucleation around ash particles (Adam Duran, oral commun., 2006). Ash from three or perhaps four of the six clouds fell entirely into Cook Inlet (events 5–7 and possibly event 3). In addition to ash fall on surrounding communities soon after these explosions, airborne ash clouds from the events took circuitous routes following high-level wind patterns. Back trajectories of the NOAA HYSPLIT wind-forecast model suggest that ash fell in northern California (January 16), communities on the southern Kenai Peninsula (January 17 and 19), Anchorage (January 19), and Palmer (January 31) because of recirculating plumes containing residual ash generated by explosive events of January 13–14.

We could not differentiate individual distal deposits from events 3–8 because they overlap and form a composite layer (table 1). The cumulative distal deposit was as much as 1 mm thick, gray-brown in color, and composed of fine to medium ash (table 3, fig. 9). Distal ash contains clear, brown, and hybrid glass shards.

Oblique aerial photographs of the island taken during a January 16 overflight show a continuous, distinctive dark-brown tephra deposit covering fresh snow on the north, east, and south flanks (fig. 3). In contrast, clean white snow on the west flank suggested little to no tephra deposition on that quadrant of the island. During August 2006, proximal ash-fall

deposits from these events were chiefly preserved on the volcano's north, northeast, east, and southeast flanks but were most voluminous on the eastern sector of Augustine Island.

Except in a few locations where primary stratigraphy is preserved (fig. 3, station KW026), we are unable to differentiate proximal deposits from the six discrete explosions. Total deposit thicknesses range from 5 to 185 cm. Thicker accumulations (on the eastern flank, fig. 10*B,* and fig. 3, stations KW034, KW078) are clearly wind and water reworked, and 5 cm is a representative thickness value for proximal, primary deposits (table 3; fig 3, station KW023; fig. 10*A*). Proximal tephra consists of light-gray, fine ash to medium lapilli (table 3). Light-gray, well-sorted, fine-ash deposits were documented on the north flank, in addition to coarse-grained deposits. Together, these deposits contain the first clear evidence of juvenile material since the start of the eruption. Such evidence includes abundant fresh-looking, angular clasts, vesicular ash and lapilli, and unaltered glass

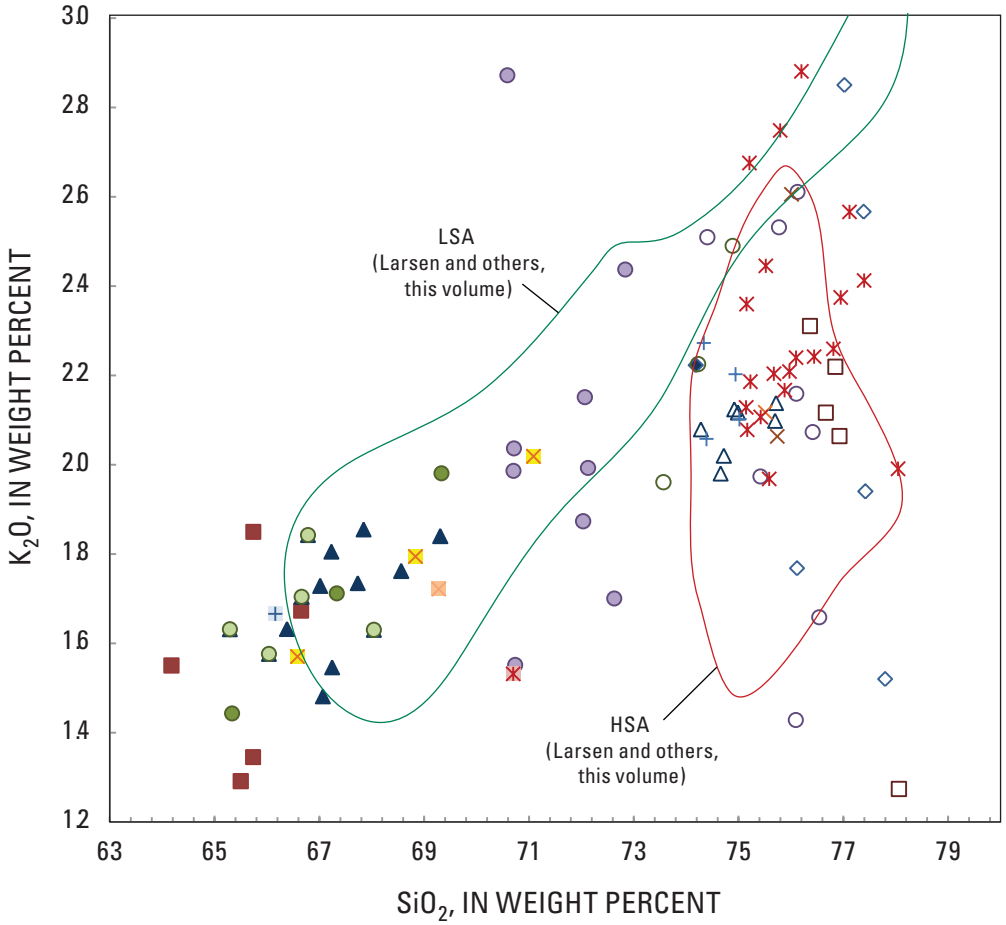

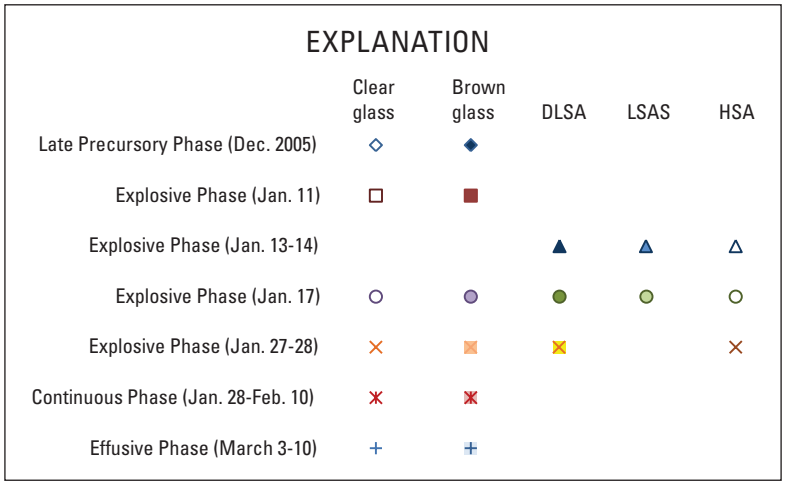

Figure 7. Plot of weight percent SiO_2 versus K_2O from microprobe analysis of groundmass (matrix) glass and glass shards for 2005–6 Augustine tephra-fall deposits. Data are separated by phase of eruption and by lithology. DLSA, dense low-silica andesite; LSAS, low-silica andesite scoria; HSA, high-silica andesite. Note that clear glass shards and HSA matrix glasses have more evolved and restricted compositions (74-78 wt. percent SiO_2), whereas brown glass shards and low-silica andesite matrix glasses have a wider range of compositions (64-74 wt. percent SiO_2). Low-silica andesite (LSA) and high-silica andesite (HSA) fields show matrix glass compositions of 2006 pyroclasts from Larsen and others (this volume).

Table 3. Summary of basic tephra-deposit characteristics for the 2005–6 eruption of Augustine Volcano.

[Maximum recorded thickness on Augustine Island (proximal thickness) was determined in July–August 2006, 6 months after the eruption ended. Maximum recorded thickness of tephra deposits on land surfaces off Augustine Island (distal thickness) was determined near the time of deposition. Bulk particle size for proximal tephra deposits uses volcanic terminology (Fisher, 1961; Schmid, 1981; Chough and Sohn, 1990): c, coarse; m, medium; f, fine. All distal deposits contain f. ash - m. ash. Componentry, in percent of clasts >5mm: HSA, high-silica andesite, gray–white pumices; DLSA, dense low-silica andesite, black–dark gray clasts; LSAS, low-silica andesite scoria; greenish-gray; banded clasts are typically pumiceous and contain gray and white/cream bands; LF, lithic fragments are nonjuvenile accidental clasts. n, number of clasts used to average componentry data; nd, no data. Componentry is from coarse-grained proximal deposits; no data from deposits with only fine-grained tephra.]

Eruption phase and date	Event no.	Max. proximal thickness, in cm	Max. distal thickness, in mm	Particle size range	HSA	DLSA	LSAS	Banded	LF	n
					Componentry					
Precursory Phase										
December 2005		0.2	0		nd	nd	nd	nd	nd	nd
Explosive Phase										
January 11, 2006	1–2	nd	3	f.ash–m. lapilli	nd	nd	nd	nd	nd	nd
January 13-14	3–8	180	1	f.ash–c. lapilli	26	22	41	2	9	475
January 17	9	1	3	f.ash–c. lapilli	35	32	20	2	11	977
January 27-28	10–13	5	1	f.ash–m. lapilli	52	18	8	8	14	215
Continuous Phase										
January 28-Feburary 10		5	1	f.ash–m. ash	60	13	6	13	8	195
Effusive Phase										
March 3-March 16		2	<1	f.ash	nd	nd	nd	nd	nd	nd

as determined by scanning electron microscopy (fig. 5). We identify four juvenile lithologies in the coarse-grained deposits (1) porphyritic, dense (black to dark gray), low-silica andesite (herein called dense low-silica andesite), (2) scoriaceous (greenish-gray), low-silica andesite (herein called low-silica andesite scoria), (3) porphyritic, pumiceous, high-silica andesite (light gray to white) (herein called high-silica andesite), and (4) banded clasts of varying textures and colors but predominantly pumiceous (fig. 5).

Componentry of undifferentiated fall deposits is 41 percent dense low-silica andesite, 22 percent low-silica andesite scoria, 26 percent high-silica andesite, 2 percent banded clasts, and 9 percent nonjuvenile lithic fragments (table 3). Glass compositions range from 66 to 69 wt. percent SiO_2 for low-silica andesite lapilli clasts and from 74 to 76 wt. percent SiO_2 for high-silica andesite (table 2 and fig. 7).

Deposits on exposed, nonvegetated slopes are most prone to reworking by wind and water (fig. 3, stations KW034, KW078, and fig. 10*B*). Deposits found in alder stands are largely unaffected by high winds and surface runoff, and outcrops of fine ash draped on branches were preserved some six months after deposition (fig. 3, station KW082, and fig. 10*C*). Figures 10*C*, *D* and *G* show only modest postdepositional modification resulting from slow melting of snow under and overlying the deposits. Distal tephra-fall deposits are not likely to be preserved in the geologic record, and certainly not as an identifiable discrete layer, because ash fall emplaced directly onto snow is remobilized during subsequent melting.

January 17, 2006 (Explosive Event 9)

Explosive event 9 on January 17 produced a plume as high as 13.5 km asl (Schneider and others, 2006) that dispersed to the west-northwest. Ash fall was first observed the same day by residents in villages surrounding Lake Iliamna, 50–120 km from Augustine (fig. 1). Observers described the deposit as a very thin dusting (<1 mm) of dark-colored ash. During field work in March 2006, the event 9 deposit formed a prominent and fairly continuous layer in the snowpack that ranged from a dark-colored discrete layer, 1–3 mm thick, to a disseminated layer over a depth of 0.5–3 cm within snow (fig. 8). Distal ash fall contains brown, fine to medium ash

with clear, brown, and hybrid glass shards. Glass compositions are in the range of 71–73 and 75–77 wt. percent SiO_2 for brown and clear glass, respectively (table 2, and fig. 7).

Proximal tephra deposits from event 9 crop out on the western sector of the island (figs. 3, 4). Oblique aerial photographs of the island during an overflight of the volcano on January 17 show a distinct dark brown deposit on the western flank and in the area within 3 km of the summit. A new lava dome, first identified during an overflight on January 16, was partially destroyed by the January 17 explosion, leaving a large crater in the new dome (Coombs and others, this volume). Observers on an overflight on January 18 identified

Figure 8. Photograph showing two distal ash layers preserved in the snow pack, 40 km west-northwest of Augustine. The lower layer is from event 1 on January 11, 2006. Event 1 tephra was deposited onto snow cover and subsequently buried by more snow. The deposit is 1–3 mm thick in this region and either discrete (shown here) or disseminated over a zone 5 mm thick. The upper layer is from event 9 on January 17, 2006, and is 1–3 mm thick in this region and either discrete (shown here) or disseminated over a zone 0.5–3 cm thick. Black cap on marker is 5 cm. Photo by Kristi Wallace, March 10, 2009.

Figure 9. Photographs showing a dusting of ash on snow and a vehicle in Homer, Alaska on January 13, 2006. Photos courtesy of Michael Fairbanks.

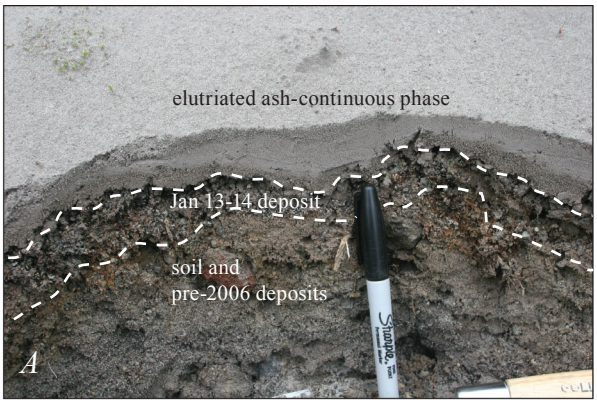
elutriated ash-continuous phase
Jan 13-14 deposit
soil and
pre-2006 deposits
A


B


C


D

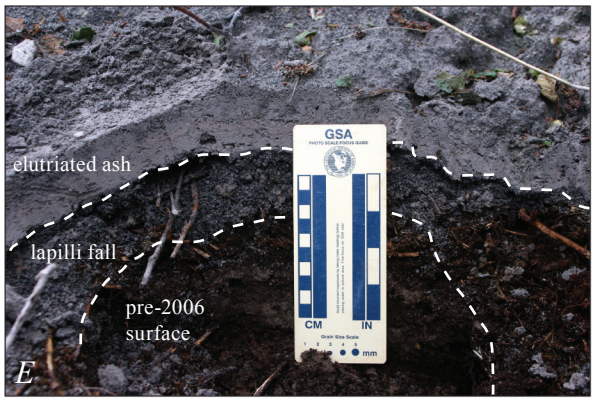
elutriated ash
lapilli fall
pre-2006
surface
GSA
CM
IN
mm
E

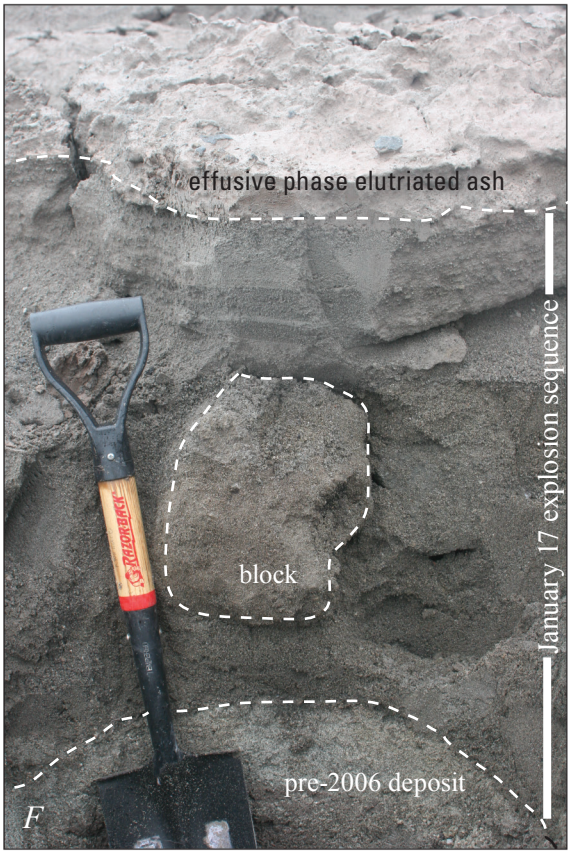
effusive phase elutriated ash
block
pre-2006 deposit
January 17 explosion sequence
F


G

a ballistic field on the upper west flank, extending 760 m from the vent (fig. 3, station KW049, and fig. 11).

Proximal deposits observed in August 2006 range from 1 to 65 cm thick (4 and 1 km from the vent respectively) and include fine ash to coarse lapilli (fig. 3, stations KW082 and KW037, fig. 10*C*, *F*). Proximal deposits contain the same lithologies seen in deposits from events 3–8: (1) 32 percent dense low-silica andesite, (2) 20 percent low-silica andesite scoria, (3) 35 percent high-silica andesite, (4) 2 percent banded clasts, and (5) 11 percent nonjuvenile lithic fragments (table 3). Glass compositions range from 65 to 69 and from 74 to 75 wt. percent SiO_2 for low-silica andesite and high-silica andesite, respectively (table 2 and fig. 7).

The tephra deposit from this event is well preserved in alder stands low on the west flank of the island and in one primary, near-vent (1 km) deposit on a bench on the upper west flank (fig. 3, stations KW082 and KW037, fig. 10*C, F*). All other exposures on nonvegetated slopes are wind and water reworked.

January 27–28, 2006 (Explosive Events 10–13)

On January 27–28, four explosions produced ash plumes between 3 and 10.5 km asl (Schneider and others, 2006) and caused ash fall on Afognak and Kodiak Islands, as far as 185 km to the southeast and south-southwest of Augustine (fig. 1). Distal ash fall was reportedly minor, with less than 1 mm of accumulation on snow. Distal deposits contain brown, fine ash with clear, brown, and hybrid glass shards, and glass compositions range from 69 to 76 wt. percent SiO_2 (table 2 and fig. 7).

Direct observations of proximal tephra deposits from this time period were not possible immediately following their emplacement because of persistent airborne ash around the island during the continuous eruptive phase that began immediately after event 13. However, proximal deposits on the south flank are attributed to events 10–13, because those plumes were the only ones during the eruption that traveled in that direction. Proximal tephra deposits on the southern sector of the island are 1–5 cm thick and contain fine ash to medium lapilli (table 3; fig. 3, station KW032; fig. 4, and fig. 10*E*).

Componentry of these undifferentiated fall deposits is 18 percent dense low-silica andesite, 8 percent low-silica andesite scoria, 52 percent high-silica andesite, 8 percent banded clasts, and 14 percent lithic fragments (table 3). Glass compositions range from 66.5 to 72 wt. percent SiO_2 for low-silica andesite and from 76 to 77 wt. percent SiO_2 for high-silica andesite (table 2 and fig. 7). Proximal fall deposits on the north sector of the island are 1–5 cm thick, contain well-sorted, gray fine ash, and are considered to be elutriate from pyroclastic flows emplaced to the north on January 27 (fig. 3, station KW070, and fig. 4) (Coombs and others, this volume). Elutriate deposits from January 27–28 are indistinguishable from elutriate deposits from the continuous eruptive phase that immediately followed the emplacement of these deposits.

Origin of Explosive Phase Tephra

The explosive phase was characterized by discrete, short-duration (1–11 minutes) explosions that produced ash plumes with tops from 4 to 14 km asl (Schneider and others, 2006) and small-volume tephra deposits (table 1). Strong seismic (McNutt and others, this volume) and infrasonic (Peterson and others, 2006) signals accompanied individual explosions; the first explosive event was preceded by a series of volcano-tectonic earthquakes on January 10 and 11 (Buurman and West, this volume; Power and Lalla, this volume; Power and others, 2006). These observations suggest a Vulcanian-style eruption mechanism (Morressey and Mastin, 2000).

Despite the general similarity among the 13 events of the explosive phase, there are some important differences. Events 1 and 2 were relatively short (1:18 and 3:18 minutes) with impulsive seismic and infrasonic signals. Unlike later events, these generated only small-volume, mixed-rock-and-snow avalanches but no pyroclastic flows (Coombs and others,

Figure 10. Photographs showing the condition and preservation of proximal tephra-fall deposits on Augustine Island from the 2005–6 eruption. *A*, Primary tephra deposit on the east flank with coarse ash to fine lapilli base from January 13–14 explosions capped by fine gray ash from the elutriation of pyroclastic flows and rockfalls, black cap on marker is 5 cm (fig. 3, KW023). *B,* Thick accumulation of wind and water reworked tephra from the January 13–14 explosions on the east flank; shovel is 60 cm long (fig. 3, KW034). *C*, Tephra preserved in an alder stand on the west flank, showing only minimal reworking; the deposit remains draped on tree branches after melting out from snow cover. Silver and orange markings on trowel handle are 1.5 cm each (fig.3, KW082). *D*, Fall deposit on the south flank, attributed to explosive events 10–13. Coarse lapilli clasts projecting out of fine-ash deposit (white arrows) indicate that fine ash deposits are thinner than maximum lapilli axes. Black cap on marker is 5 cm (fig 3, KW084). *E*, Lithic lapilli fall of low-silica andesite deposit (January 27–28 explosions) on the south coast of Augustine capped by fine elutriated ash from the continuous and effusive phases (fig. 3, KW032). *F*, Near vent exposure of January 17 tephra-fall deposit on the upper west flank, including a ballistic block; shovel is 60 cm long (fig. 3, KW037). *G,* Typical exposure of a tephra deposit overlying leaf litter and a well-defined organic layer in alder stands on Augustine Island. Pre-2006 tephra deposits underlie the organic horizon (fig. 3, KW063). All photos by Kristi Wallace, August 7, 2006.

this volume). Plumes from events 1 and 2 appear to have contained low concentrations of ash and only deposited very thin, localized tephra. Proximal deposits from these events are dominated by dense and altered material. Distal tephra deposits do contain glass with intermediate to silicic glass compositions. Because of the similar compositions of matrix glasses between juvenile 2006 tephra and that from the 1976 and 1986 eruptions, however, it is impossible to know if the analyzed shards are new 2006 material or recycled from previous eruptions. On the basis of other lines of evidence, we think that the glass in the distal January 11 ash may be recycled. This was also the case for ash from the 2004–5 eruption of Mount St. Helens, where clean glass in distal ash was determined to have derived from nonjuvenile sources (Rowe and others, 2008). Because events 1 and 2 contained little or no juvenile material, they were likely caused when gases at the top of the ascending magma body reached the surface (Larsen and others, this volume). Interestingly, event 11 on January 27 had a similar seismic signal (McNutt and others, this volume), a low ash signal in radar (Schneider and others, 2006), and may have formed by a similar process, although its deposits were not uniquely identified.

Vulcanian explosions of January 13–14 (events 3–8) generated plumes 10–16 km asl and column-collapse pyroclastic flows that spread radially on all sides of the volcano, as well as secondary lahars and mixed snow and rock avalanches (Vallance and others, this volume). Tephras from these events are dominated by low-silica andesite (63 percent), with lesser amounts of high-silica andesite, lithics, and banded clasts (table 3). The succession of six discrete explosive plumes within less than 24 hours suggests rapid ascent of magma to the surface. Following event 8, a low-silica andesite lava lobe effused at the summit (Coombs and others, this volume; Larsen and others, this volume).

On January 17, after a 3-day pause in explosive activity, a Vulcanian explosion (event 9) produced one of the highest

Figure 11. Photograph illustrating ballistic field near the summit of Augustine, upper west flank (fig.3, KW049). Fine ash generated from pyroclastic flows and rockfalls during the effusive phase drape ballistic blocks on the surface. New dome steaming in the background. Note circled figure for scale. Photo by Kristi Wallace, August 2006.

plumes of the eruption sequence (table 1). Like tephra from the January 13–14 events, event 9 tephra was predominantly low-silica andesite (52 percent), but deposits have slightly higher proportions of high-silica andesite compared to January 13–14 events (table 3). Low-silica andesite lapilli closely resemble the low-silica andesite of the new lava lobe in texture and composition (Coombs and others this volume; Larsen and others, this volume). The new lava dome probably sealed the vent and allowed pressure to build until it ruptured, and explosive decompression of gas-rich magma generated a vigorous plume.

Vulcanian explosions of January 27 and 28 (events 10–14) occurred after a 10-day hiatus in explosive events. Between January 17 and 27, a new high-silica lava-dome lobe grew at the summit (Coombs and others, this volume; Larsen and others, this volume). In coarse-grained fall deposits from events 10–13, high-silica andesite lithologies predominate (52 percent) and closely match the composition of the January 17–27 dome. Subordinate low-silica andesite is more commonly dense and black to dark gray rather than scoriacious (table 3). In addition to vent explosions that resulted in relatively coarse fall deposits, fine elutriated ash from large pyroclastic flows of January 27 (Coombs and others, this volume) fell on the north flank of the volcano. These fine-ash deposits are indistinguishable from continuous phase deposits (see below) in terms of predominance of high-silica andesite shards.

The succession of magma compositions throughout the explosive phase from low-silica to high-silica andesite, as shown in tephra-deposit componentry, is also seen in componentry of pyroclastic-flow deposits (Vallance and others, this volume). Petrological studies (Larsen and others, this volume; Webster and others, this volume) suggest that mixing between an old shallow (4–6 km below the surface) high-silica andesite magma and a deep, young mafic end member (basalt) produced the low-silica andesite that was predominantly erupted during the early explosive phase (January 13, 14, and 17). The high-silica andesite that predominated in the late explosive phase (January 27 and 28) was likely remobilized by the injection of the mafic magma, allowing it to rise to the surface (Larsen and others, this volume).

Continuous Phase Tephra Deposits (January 28–February 10, 2006)

Distribution and Character of Continuous Phase Tephra

The continuous phase of the eruption lasted from January 28 through February 10 and was characterized by constant low-level ash emissions from the summit vent (plume heights <4 km asl), emplacement of pyroclastic flows on the north flank that generated clouds of elutriate ash, and discrete explosions generating ash plumes between 3 and 7 km asl (Schneider and others, 2006). Persistent north winds dispersed ash to the south-southeast over this 2-week time period and ash fall occurred in communities on Afognak and Kodiak Islands, as far as 185 km from Augustine, on February 1 and 3 (fig. 1). Proximal tephra deposits blanketed all sectors of the volcano, but predominated on its northern flank.

Photographs taken during observational overflights on January 29 and 30 show a continuous plume of ash and steam rising from the summit of the volcano (fig. 12). The plume was light colored, which suggests low concentrations of ash compared to plumes of the explosive phase. Discrete explosions during this phase have durations and plume heights similar to those produced during the explosive phase (table 1), and we infer by analogy that such plumes contained higher concentrations of ash than at other times during this phase. Photographs taken on January 30 and February 3 show tephra fallout from two sources. The first is a plume extending downwind from the vertical eruption column rising from the summit vent (labeled A in fig. 12). The second is a cloud of elutriated ash generated during emplacement of pyroclastic flows on the north flank of the volcano (labeled B in fig. 12) (Coombs and others, this volume). This second ash cloud was distinctly brownish pink compared to the light gray, ash-poor plume originating at the vent. Observations of fall deposits on the island during overflights were hindered by the lack of visibility owing to the haze of suspended fine ash surrounding the erupting volcano.

Distal ash reportedly fell as a mixture of ash and snow during a snowstorm. Distal tephra deposits were light gray and contained minor amounts of ash. Cumulative ash fall on Kodiak Island was less than 1 mm thick. Distal samples contain brown, clear, and hybrid glass. Glass compositions range from 75 to 77 wt. percent SiO_2 for clear glass and from 66 to 69.5 wt percent SiO_2 for brown glass (table 2 and fig. 7).

Proximal fall deposits were widely distributed over Augustine Island. Coarse-grained tephra (lapilli) deposits, presumably originating from discrete explosions or from the continuous plume generated at the vent, are located mainly in the southern sector of the island where they overlie elutriate deposits (fig. 3, stations KW030 and KW032; fig. 4). Coarse tephra deposits range from 1 to 5 cm in thickness and contain 60 percent high-silica andesite, 13 percent dense low-silica andesite, 6 percent low-silica andesite scoria, 13 percent banded clasts, and 8 percent lithic fragments (table 3). Light gray fine ash associated with pyroclastic flows was deposited on all sectors of the volcano but is thickest (as much as 2 cm) on the north and south flanks (figs. 4 and 12). Elutriated fine ash deposits grade upward to overlying effusive phase deposits, which can be distinguished by their pale pinkish-orange color (figs. 12 and 13).

Origin of Continuous Phase Tephra

Steady extrusion of a high-silica andesite dome, numerous column- and dome-collapse pyroclastic flows and rock falls (Coombs and others, this volume), continuous low-level ash emissions (<4 km asl), and occasional discrete vent explosions characterized the continuous phase (January 28–Feburary 10, 2006). Seismicity during this time is consistent with steady magma ascent and extrusion at the surface (Power

and Lalla, this volume). Discrete explosions produced plumes as high as 7.2 km asl and large pyroclastic flows (Coombs and others, this volume). Transient overpressures from sealing of the vent by high-silica andesite lava may have caused such bursts of energetic activity. High-silica andesite is the most common lithology in the fall deposits—consistent with explosive disruption of a high-silica andesite dome (table 2). Numerous continuous-phase pyroclastic flows generated low-level plumes of fine ash that drifted downwind and draped surroundings with fine-grained tephra deposits.

Continuous-phase fine-grained elutriated ash deposits contain a high proportion of clear glass shards, whose composition is consistent with the high-silica andesite dome and flows.

Effusive Phase Tephra Deposits (March 3–16, 2006)

Distribution and Character of Effusive Phase Tephra

On March 3, eruptive activity resumed after a brief hiatus (21 days) with the effusion of a low-silica andesite summit lava dome and lava flows that descended to the north and northeast, together with a coincidental increase in rock-fall activity (Coombs and others, this volume; Power and Lalla, this volume). Time-lapse photography and aerial observations revealed that elutriation of fine ash from rockfalls and small pyroclastic flows generated low-level ash clouds (<3 km asl). Fall deposits include localized fine ash on the north flank of

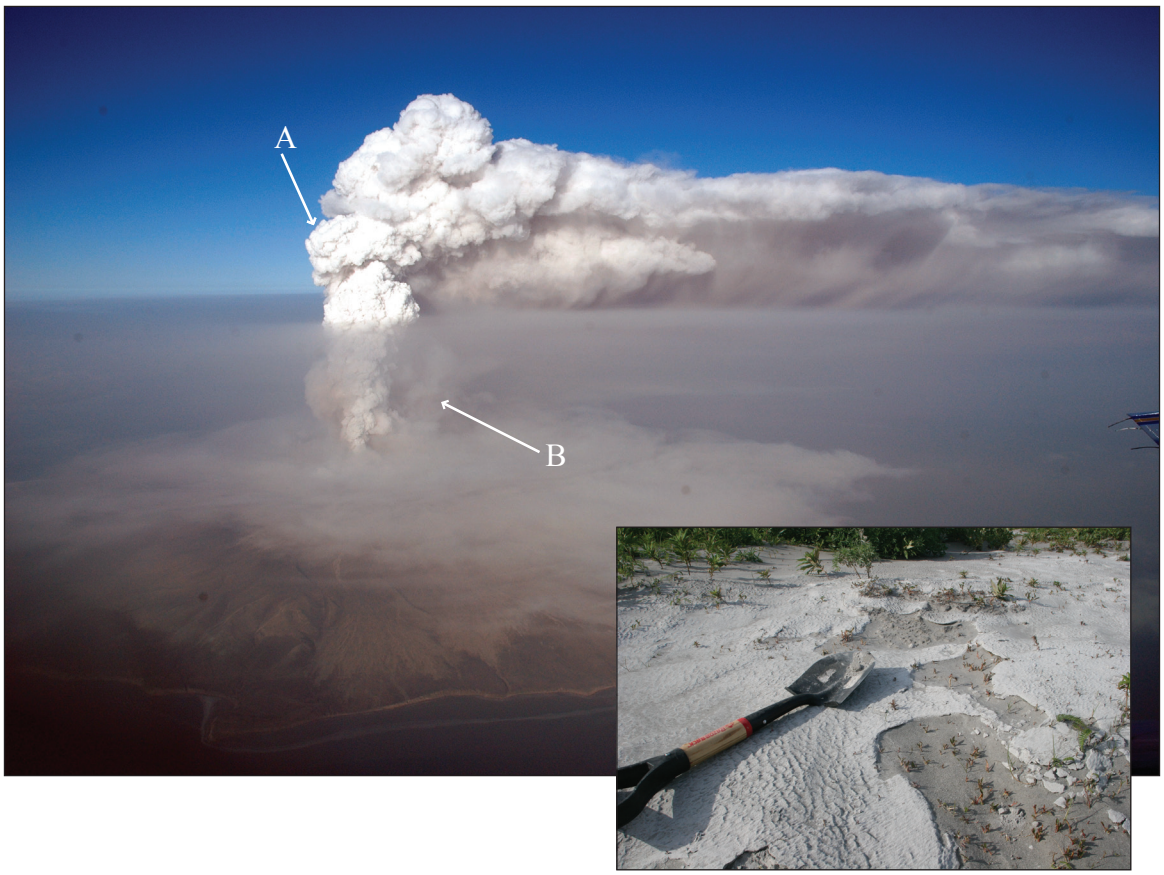

Figure 12. Photograph from an observation flight on January 30, 2006, showing tephra from two sources: *A*, a plume 10-15 km asl extending northeast from the vertical eruption column rising from the summit vent, and *B*, clouds of elutriated ash generated from newly emplaced pyroclastic flows on the north flank of the volcano. View from south. Photo by R.G. McGimsey. Inset photograph shows a typical exposure of a fine-ash deposit elutriated from pyroclastic flows on the north side of the island (fig.3-KW071). Shovel is 60 cm long. Photo by Kristi Wallace, August 6, 2006.

the volcano. Although radar or satellite imagery identified no significant ash clouds, on March 11 and 20, during a period of high easterly winds, minor ash fall was reported at the village of Pope Vanoy, near Lake Iliamna, 85 km west-northwest of Augustine (fig. 1).

Distal deposits were reportedly fine dustings of ash, clearly visible on fresh snow. A distal sample contains brown, clear (abundant), and hybrid glass shards. Glass compositions range from 68 to 78 wt. percent SiO_2 (appendix 2, sample AT-770). Proximal deposits are as much as 2 cm thick and contain fine, pinkish brown, well-sorted ash (fig. 13) with glass compositions ranging from 64 to 75 wt. percent SiO_2 (table 2 and fig. 7). Proximal tephra contains brown (abundant), clear, and hybrid glass shards. No explosions from the vent are thought to have occurred during this time.

Origin of Effusive Phase Tephra

Low-level plumes were generated from small pyroclastic flows and rock falls from the actively growing low-silica andesite lava dome and lava flows (Coombs and others, this volume; Power and Lalla, this volume). Tephra deposits are minor and were caused by the elutriation of fine ash from these small, gravitational collapses of the dome and from lava-flow fronts, either as minor rockfalls or block-and-ash flows. The pinkish brown color of elutriate ash deposits probably results from its more mafic composition (and higher proportion of brown glass shards) and possibly from oxidation. Clear, silicic glass shards, however, predominate in distal tephra deposits, which is inconsistent with the composition of the low-silica andesite dome being extruded during this time. Strong easterly winds reported during this interval likely remobilized unconsolidated fine material from the voluminous high-silica andesite pyroclastic-flow deposits on the north flank that were generated during the late explosive phase (Coombs and others, this volume) and carried it westward to the Iliamna area.

Mass of Select Tephra Deposits

Ideally, the total mass of tephra-fall deposits can be used to estimate the volume of magma that was explosively erupted and transported as ash clouds. Such data could not be obtained for all ash clouds generated during the Augustine 2005-6 eruption because of deposition (1) into Cook Inlet, (2) onto uninhabited and sparsely inhabited areas, and (3) of small volume, fine-grained ash onto seasonal snow pack and subsequent reworking. In addition, mixing of successive layers presented a problem for the six ash clouds generated on January 13 and 14, which fell onto land northeast of the volcano. Of the 13 tephras generated during the explosive phase, only that of January 17 was suitable for mass and volume calculation. Our estimates are based on 10 mass-per-unit-area measurements from this single deposit (figs. 14 and 15). On the basis of similarities in scale and assumed eruption mechanism to the other discrete ash clouds generated during the explosive phase, we use mass values from the January 17 deposit to extrapolate mass and volume values for the other events of the explosive phase (table 1 and 4). We do not estimate volumes of elutriated ash fall from pyroclastic flows.

The total mass for the January 17 tephra-fall deposit is estimated at 1.73×10^9 kg (fig. 14), with a bulk volume of 1.73×10^6 m^3 and a DRE volume of 6.65×10^5 m^3 (table 4). Total mass of tephra fall from the 13 discrete plumes generated during the explosive phase is calculated by multiplying the cumulative seismic duration by the mass eruption rate (calculated from the January 17 plume), which results in 2.2×10^{10} kg. Total bulk volume is 22×10^6 m^3 and total dense-rock equivalent (DRE) volume is 8.5×10^6 m^3 (table 4). These values are modest in comparison to tephra-fall volumes from previous historical eruptions of Augustine (Pyle, 2000; Venzke and others, 2002).

Significance and Hazards of Tephra-Fall Events

Although eruption parameters such as timing, magma composition, and total volume of erupted products for this eruption are much like those observed in past eruptions of Augustine, total vent explosion tephra-fall volume is about one order of magnitude smaller than estimates for the 1976 and 1986 eruptions (Pyle, 2000; Venzke and others, 2002). Historical eruptions of Augustine had a Volcanic Explosivity Index (VEI) of 4 (Venzke and others, 2002), but we assign the 2005–6 eruption a VEI of 3 on the basis of maximum plume height of 13.5 km (event 7 and 9). A VEI is typically weighted on both plume height and volume of tephra fall, but because of the overall lack of volume data for this eruption, we assign a VEI of 3 based on the explosion with the highest plume (L. Siebert, Smithsonian Institute, Global Volcanism Program, written commun., 2006). The 2005–6 eruption of Augustine produced about one order of magnitude less tephra fall than recent eruptions of Cook Inlet volcanoes Redoubt and Spurr (see, for example, Miller and others, 1998; Scott and McGimsey, 1994; McGimsey and others, 2001). Other volcanoes with similar Vulcanian-style eruption mechanisms, such as Unzen, Soufriere Hills, Vulcano, Ngauruhoe, Irazu, and Sakurajima, have tephra-fall volumes (individual events as well as cumulative over an eruptive episode) that are comparable within one order of magnitude (Bonnadonna and others, 2002; Herd and others, 2005; Venzke and others, 2002) to the 2005–6 eruption of Augustine.

Although the potential threat of ash fall was a significant concern during the eruption, the end result was that ash fall was not a significant problem in communities surrounding the volcano (fig. 1). Tephra fall was one of AVO's main concerns for surrounding communities, and the public

mirrored these concerns through consultation of AVO's Web site and public communications (Adleman and others, this volume). Satellite imagery, NOAA HYSPLIT wind-model data, and ash-plume and fall modeling aided AVO in tracking and projecting ash-plume movement and, furthermore, assisted us in briefing the public about the likelihood and nature of tephra fall throughout the eruption. The only reports of health effects from ash fall were as a minor eye irritant on two occasions (aircraft encounters on January 14) and as a nose irritant on one occasion (January 17, Iliamna). Air-quality samplers of fine particulate matter (PM) operated by the Municipality of Anchorage (MOA) and the Department of Environmental Conservation (DEC) detected elevated levels of PM_{10} and $PM_{2.5}$ (<10 and 2.5 microns, respectively) in Anchorage, Soldotna, and Homer during the eruption. Nevertheless, fine particulate levels never exceeded Environment Protection Agency (EPA) air quality standards (fig. 16). Particles 10 microns (that is, PM_{10}) in diameter and smaller can be inhaled into the respiratory tract, where they can cause harm (C. Cahill, oral commun., 2006). On January 13, ash accumulation as thick as 1 mm in Homer probably exceeded the amounts for all other days when instruments were deployed. The small volumes of individual ash-fall deposits make it unlikely that ash caused environmental impacts to water supplies, and no such impacts were reported.

Figure 13. Photograph from an observation flight on March 6, 2006, showing generation of an ash cloud from a small block-and-ash flow associated with dome collapse during the effusive phase. Photo courtesy of Guy Tytgat. Inset photograph (fig.3, KW049) shows, (A), a fine pinkish-brown ash deposit associated with the effusive phase, (B), a fine gray oxidized ash deposit associated with the continuous phase, and (C), a coarse proximal tephra-fall deposit associated with the continuous phase. Both A and B were generated from pyroclastic flows, while C was generated from a vent explosion. Photo from the upper northwest flank of the volcano. Trowel is 25 cm long. Photo by Kristi Wallace, August 2006.

Table 4. Summary of mass and volume data for explosive-phase plumes from Augustine Volcano, January 11–28, 2006.

[Events 1 and 2 contain little juvenile material, so mass and volume calculations likely represent pre-2006 ejecta. Duration of seismic signal at distal seismic station Oil Point (OPT) (fig. 1; Power and Lalla, this volume) used as a proxy for time of plume generation. Mass of tephra fall is based on mass eruption rate for event 9 on January 17, 2006: 6.9×10^6 kg/sec. Bulk volume in cubic meters (m^3) calculated using a density of 1,000 kg/m^3. Dense-rock-equivalent (DRE) volume in cubic meters calculated using a density of 2,600 kg/m3.]

Event date, in AKST (UTC)	Event no.	Seismic duration at OPT, in min:sec	Mass, in 10^9 kg	Bulk volume, in 10^6 m^3	Dense-rock-equivalent volume, in 10^6 m^3
1/11/06	1	01:18	0.5	0.5	0.2
1/11/06	2	03:18	1.4	1.4	0.5
1/13/06	3	11:00	4.6	4.6	1.8
1/13/06	4	04:17	1.8	1.8	0.7
1/13/06	5	03:24	1.4	1.4	0.5
1/13/06 (01/14/06)	6	04:00	1.7	1.7	0.6
1/13/06 (01/14/06)	7	03:00	1.2	1.2	0.5
1/14/06	8	03:00	1.2	1.2	0.5
1/17/06	9	04:11	1.7	1.7	0.7
1/27/06 (01/28/06)	10	09:00	3.7	3.7	1.4
1/27/06	11	01:02	0.4	0.4	0.2
1/28/06	12	02:06	0.9	0.9	0.3
1/28/06	13	03:00	1.2	1.2	0.5
Total			**21.7**	**21.7**	**8.4**

Conclusions

Tephra fall from the 2005–6 eruption of Augustine occurred during each of four eruption phases. Phreatic explosions during the late precursory phase produced little ash fall and posed no hazard to local communities. Initial eruption of low-silica andesite mixed with subordinate high-silica andesite magma initiated a series of 13 discrete Vulcanian explosions during the explosive phase, which generated plumes from 4 to14 km asl and distributed ash 25–185 km from the volcano in all directions. Minor ash fall of ≤1 mm resulted and posed little hazard to local communities. The hazard to aviation was mitigated by monitoring efforts of the AVO and NWS. During the late explosive phase and continuous phase, a dome of high-silica andesite composition was extruded. Subsequent collapses of the dome generated voluminous pyroclastic flows (Coombs and other, this volume), which generated ash clouds (<4 km asl) by elutriation. The resulting tephra deposits are localized to and distributed all over the island (fig. 4). Tracking ash during this phase was hindered by the continuous, long-duration emission of fine-grained low-volume ash clouds. A return to the eruption predominantly of low-silica andesite magma during the effusive phase (Coombs and others, this volume) resulted in the emplacement of a dome and lava flows. Local ash fall associated with small collapses of the lava dome and lava flows was of limited extent and posed no hazard to local communities. Fall deposits from the 2005–6 eruption are not likely to be well-preserved in the geologic record on or off island, because of their small volume, deposition into Cook Inlet, and reworking by wind and water. Total eruption volume (Coombs and other, this volume) is comparable with past eruptions of Augustine, yet tephra-fall volumes are about an order of magnitude smaller because flowage deposits (pyroclastic flows, lava flows/domes, block and ash flows) make up the bulk of erupted products (Coombs and others, this volume). Magma heterogeneity observed throughout the eruption (fig. 7) in both whole-rock and glass compositions, and overall similarity to recent eruptions, will present challenges for future tephrostratigraphers aiming to distinguish among these and other deposits from Augustine.

Acknowledgments

We would like to thank the many residents of communities surrounding Augustine for their keen observations and sampling efforts made during this eruption. Many thanks to AVO staff for their samples and excellent, well-documented photography throughout the eruption. We thank Evan Thoms for his help with GIS map preparation. We thank Manny Nathenson for his significant contributions and helpful discussion of our mass and volume calculations. We thank Barbara Stunder of the National Weather Service for providing the HYSPLIT model, forward trajectories, and GDAS Meteorological Data shown in figure 2. We thank Rick Farrish for safely transporting us all over Augustine Island during our field campaign. We appreciate the opportunity to do fieldwork in the Iliamna region and thank the Iliamna region native councils and the National Park Service for access to this land. Special thanks to Judy Fierstein, James Vallance, and Michelle Coombs for their careful reviews and suggestions for revisions to this manuscript, which we think have increased its value significantly.

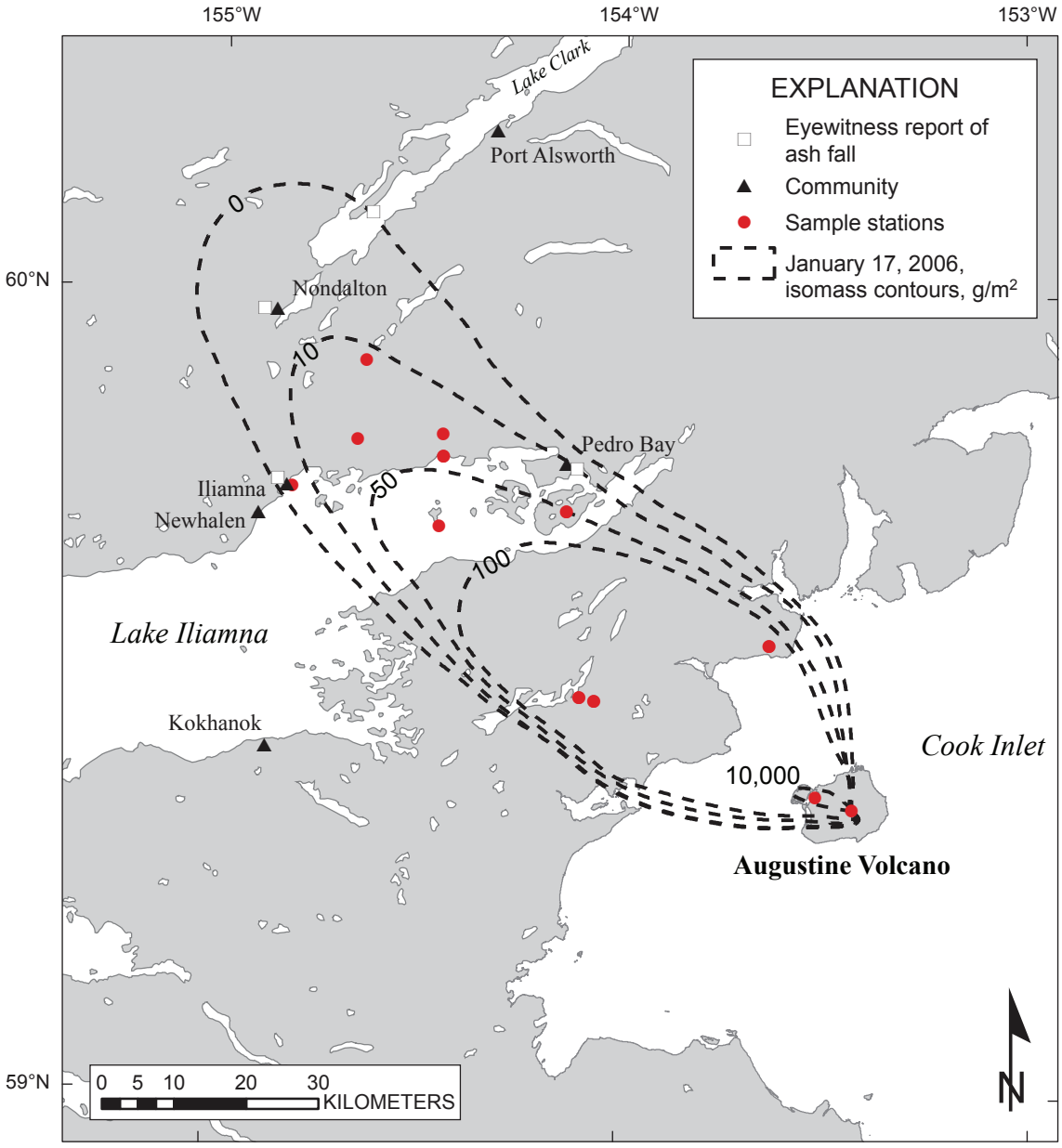

Figure 14. Isomass map of the tephra-fall deposit from Augustine on January 17, 2006. Contours represent lines of equal mass (g/m^2). Mass data were collected using measured-area sampling.

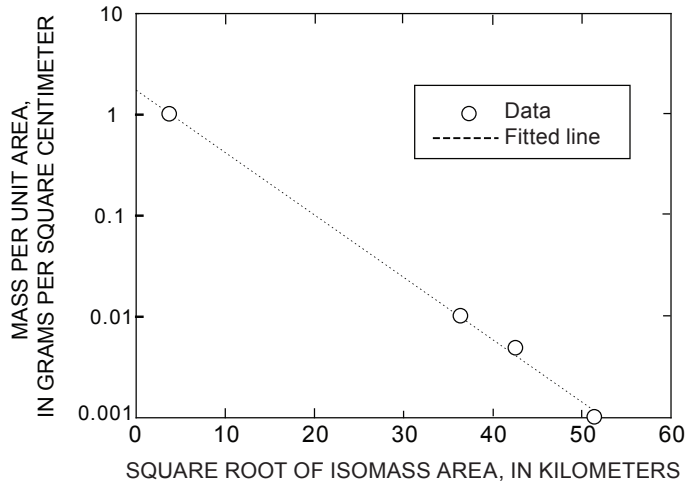

Figure 15. Plot showing mass per unit area (MPUA) versus the square root of isomass area for fall deposits from event 9 on January 17, 2006. The available data are well fitted by a single straight line for the calculation of total mass of the deposit. Tephra volume is calculated from the total mass of the deposit calculated using the root-area method (Pyle, 1989; Fierstein and Nathenson, 1992).

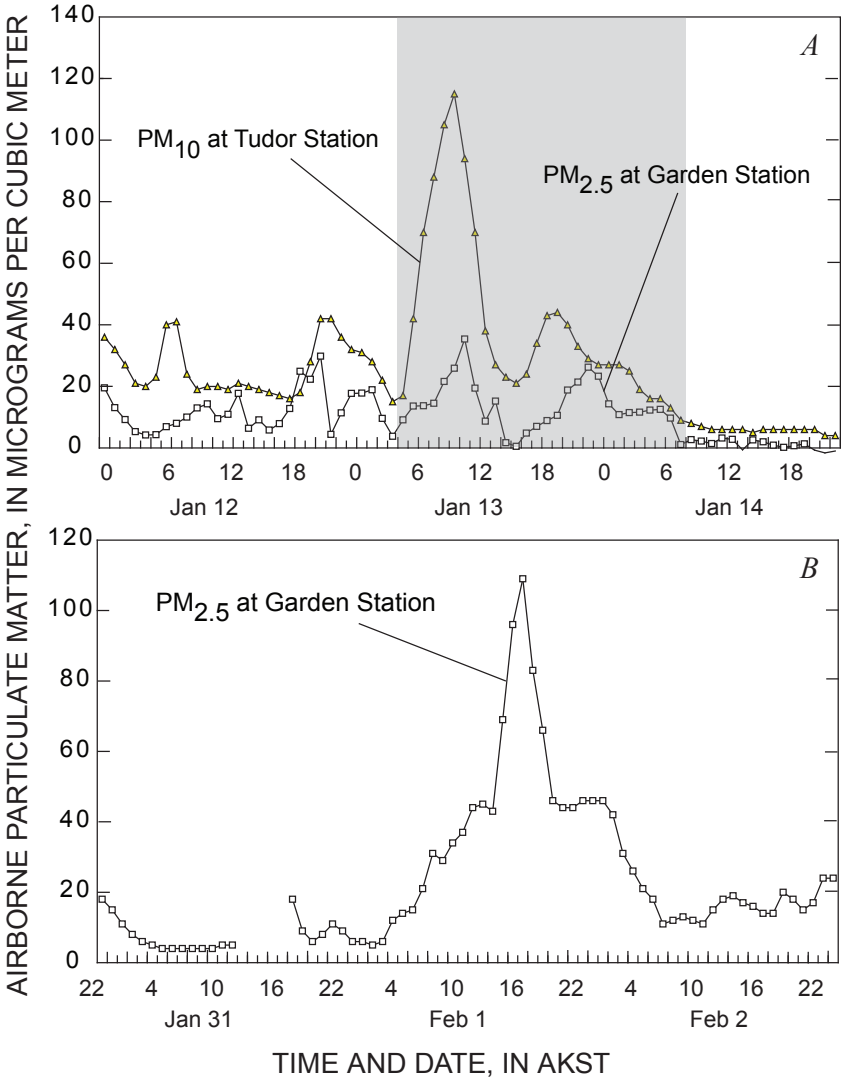

Figure 16. Plots showings airborne particulate matter (PM) in Anchorage, Alaska, on (*A*), January 12–14 and (*B*), January 31–February 2, 2006. Shaded area is the time frame when explosions occurred on January 13 and 14. PM levels however, did not exceed Environmental Protection Agency standards on these days. PM_{10}, aerodynamic diameter <10 microns; $PM_{2.5}$, aerodynamic diameter <2.5 microns. Tudor Station 3335 East Tudor Road; Garden Station, 3000 E 16th Street. Data provided by Steve Morris, Municipality of Anchorage, Environmental Services Division.

References Cited

Adleman, J.N., Cameron, C.E., Snedigar, S.F., Neal, C.A., and Wallace, K.L., 2010, Public outreach and communications of the Alaska Volcano Observatory during the 2005–2006 eruption of Augustine Volcano, *in* Power, J.A., Coombs, M.L., and Freymueller, J.T., eds., The 2006 eruption of Augustine Volcano, Alaska: U.S. Geological Survey Professional Paper 1769 (this volume).

Bailey, J.E., Dean, K.G., Dehn, J., and Webley, P.W., 2010, Integrated satellite observations of the 2006 eruption of Augustine Volcano, *in* Power, J.A., Coombs, M.L., and Freymueller, J.T., eds., The 2006 eruption of Augustine Volcano, Alaska: U.S. Geological Survey Professional Paper 1769 (this volume).

Bonnadonna, C., Mayberry, G., Calder, E.S., Sparks, R.S.J., Choux, C, Jackson, P., Lejeune, A., Loughlin, S., Norton, G, Rose, W., Ryan, G., and Young, S., 2002, Tephra fallout in the eruption of Soufriere Hills Volcano, Montserrat, *in* Druitt, T.H., and Kokelaar, B., eds., The eruption of Soufriere Hills Volcano, Montserrat, from 1995 to 1999: Geological Society of London Memoir, 21, p. 483–516.

Buurman, H., and West, M.E., 2010, Seismic precursors to volcanic explosions during the 2006 eruption of Augustine Volcano, *in* Power, J.A., Coombs, M.L., and Freymueller, J.T., eds., The 2006 eruption of Augustine Volcano, Alaska: U.S. Geological Survey Professional Paper 1769 (this volume).

Cahill, C.F., Cahill, T.A., Webley, P., Wallace, K.L., Dean, K.G., and Dehn, J., 2006, Size- and time-resolved composition of volcanic ash from Augustine Volcano, Alaska [abs.]: Eos (American Geophysical Union Transactions), v. 87, Fall meeting supp., abs. V22B-05.

Cervelli, P.F., Fournier, T.J., Freymueller, J.T., Power, J.A., Lisowski, M., and Pauk, B.A., 2010, Geodetic constraints on magma movement and withdrawal during the 2006 eruption of Augustine Volcano, *in* Power, J.A., Coombs, M.L., and Freymueller, J.T., eds., The 2006 eruption of Augustine Volcano, Alaska: U.S. Geological Survey Professional Paper 1769 (this volume).

Coombs, M.L., Bull, K.F., Vallance, J.W., Schneider, D.J., Thoms, E.E., Wessels, R.L., and McGimsey, R.G., 2010, Timing, distribution, and volume of proximal products of the 2006 eruption of Augustine Volcano, *in* Power, J.A., Coombs, M.L., and Freymueller, J.T., eds., The 2006 eruption of Augustine Volcano, Alaska: U.S. Geological Survey Professional Paper 1769 (this volume).

Chough, S.K., and Sohn, Y.K., 1990, Depositional mechanics and sequences of base surges, Songaskan tuff rings, Cheju Island, Korea: Sedimentology, v. 37, p. 1115–1135.

Daley, E.E., 1986, Petrology, geochemistry, and the evolution of lavas at Augustine Volcano, Alaska: Fairbanks, University of Alaska Fairbanks, MS thesis, 103 p.

de Fontaine, C.S., Kaufman, D.S., Anderson, R.S., Werner, A., Waythomas, C.F., and Brown, T.A., 2007, Late Quaternary distal tephra-fall deposits in lacustrine sediments, Kenai Peninsula, Alaska: Quaternary Research, v. 68, p. 64–78.

Fierstein, J., and Nathenson, M., 1992, Another look at calculation of fallout tephra volumes: Bulletin of Volcanology, v. 54, p. 156–167.

Fisher, R.V., 1961, Proposed classification of volcaniclastic sediments and rocks: Geological Society of America Bulletin, v. 72, p. 1409–1414.

Herd, R.A, Edmonds, M, and Bass, V.A., 2005, Catastrophic lava dome failure at Soufriere Hills Volcano, Montserrat, 12–13 July 2003: Journal of Volcanology and Geothermal Research, v. 148, p. 234–252.

Johnston, D.A., 1978, Volatiles, magma mixing and the mechanism of eruption of Augustine Volcano, Alaska: Seattle, University of Washington, Ph.D dissertation, 204 p.

Kienle, J., and Swanson, S. E., 1987, The 1986 activity of Mt. St. Augustine; volcanic hazards in the Cook Inlet Basin [abs.]: *in* Geologic Hazards Symposium, Alaska Geological Society Symposium Agenda and Abstracts, Anchorage, Alaska, May 12-15, 1987, unpaged.

Larsen, J.F., Nye, C.J., Coombs, M.L., Tilman, M., Izbekov, P., and Cameron, C., 2010, Petrology and geochemistry of the 2006 eruption of Augustine Volcano, *in* Power, J.A., Coombs, M.L., and Freymueller, J.T., eds., The 2006 eruption of Augustine Volcano, Alaska: U.S. Geological Survey Professional Paper 1769 (this volume).

McGee, K.A., Doukas, M.P., McGimsey, R.G., Neal, C.A., and Wessels, R.L., 2010, Emission of SO_2, CO_2, and H_2S from Augustine Volcano, 2002–2008, *in* Power, J.A., Coombs, M.L., and Freymueller, J.T., eds., The 2006 eruption of Augustine Volcano, Alaska: U.S. Geological Survey Professional Paper 1769 (this volume).

McGimsey, R.G., Neal, C.A., and Riley, C.M., 2001, Areal distribution, thickness, mass, volume, and grain size of tephra-fall deposits from the 1992 eruptions of Crater Peak Vent, Mt. Spurr volcano, Alaska: U.S. Geological Survey Open-File Report 01-0370, 38 p.

McNutt, S.R., Tytgat, G., Estes, S.A., and Stihler, S.D., 2010, A parametric study of the January 2006 explosive eruptions of Augustine Volcano using seismic, infrasound, and lightning data, *in* Power, J.A., Coombs, M.L., and Freymueller, J.T., eds., The 2006 eruption of Augustine Volcano, Alaska: U.S. Geological Survey Professional Paper 1769 (this volume).

Miller, T.P., McGimsey, R.G., Richter, D.H., Riehle, J.R., Nye, C.J., Yount, M.E., and Dumoulin, J.A., 1998, Catalog of the historically active volcanoes of Alaska: U.S. Geological Survey Open-File Report, 98-0582, 104 p.

Morrissey, M., and Mastin, L, 2000, Vulcanian eruptions, *in* Sigurdsson, H., Houghton, B.F., McNutt, S.R., Rymer, H., Stix, J., eds., Encyclopedia of volcanoes: Academic Press, p. 463–475.

Petersen, T., De Angelis, S., Tytgat, G., and McNutt, S., 2006, Local infrasound observations of the large ash explosions at Augustine Volcano, Alaska, during January 11–28, 2006: Geophysical Research Letters, v. 33, L12303, p. 1–5, doi: 10.1029/2006GL026491.

Power, J.A., Nye, C.J., Coombs, M.L., Wessels, R.L., Cervelli, P.F., Dehn, J., Wallace, K.L., Freymueller, J.T., and Doukas, M.P., 2006, The reawakening of Alaska's Augustine Volcano: Eos (American Geophysical Union Transactions), v. 87, no. 37, p. 373, 377.

Power, J.A., and Lalla, D.J., 2010, Seismic observations of Augustine Volcano, 1970–2007, *in* Power, J.A., Coombs, M.L., and Freymueller, J.T., eds., The 2006 eruption of Augustine Volcano, Alaska: U.S. Geological Survey Professional Paper 1769 (this volume).

Pyle, D.M., 1989, The thickness, volume, and grainsize of tephra-fall deposits: Bulletin of Volcanology, v. 51, p. 1–15.

Pyle, D.M., 2000, Sizes of volcanic eruptions, *in* Encyclopedia of volcanoes, Sigurdsson, H., Houghton, B.F., McNutt, S.R., Rymer, H., Stix, J., eds.: Academic Press, p. 263–269.

Riehle, J.R., 1985, A reconnaissance of the major Holocene tephra deposits in the upper Cook Inlet region, Alaska: Journal of Volcanology and Geothermal Research, v. 26, p. 37–74.

Roman, D.C., Cashman, K.V., Gardner, C.A., Wallace, P.J., and Donovan, J.J., 2005, Storage and interaction of compositionally heterogeneous magmas from the 1986 eruption of Augustine Volcano, Alaska: Bulletin of Volcanology, v. 68, p. 240–254, doi: 10.1007/s00445-005-0003-z.

Rowe, M.C., Thornber, C.R., and Kent, A.J.R., 2008, Identification and evolution of the juvenile component in 2004–2005 Mount St. Helens ash, *in* Sherrod, D.R., Scott, W.E., and Stauffer, P.H., eds. A volcano rekindled; The renewed eruption of Mount St. Helens, 2004–2006: U.S. Geological Survey Professional Paper 1750, p. 269–646.

Sarna-Wojcicki, A.M., Meyer, C.E., Woodward, M.J., and Lamothe, P.J., 1981, Composition of air-fall ash erupted on May 18, May 25, June 12, July 22, and August 7, *in* Lipman, P.W., and Mullineaux, D.R., eds., The 1980 eruptions of Mount St. Helens, Washington: U.S. Geological Survey Professional Paper 1250, p. 667.

Schmid, R. 1981, Descriptive nomenclature and classification of pyroclastic deposits and fragments; recommendations of the IUGS Subcommission on the Systematics of Igneous Rocks: Geology, v. 9, p. 41– 43.

Schiff, C.J., Kaufman, D.S., Wallace, K.L., Werner, A., Ku, T.L., 2008, Modeled tephra ages from lake sediments, base of Redoubt Volcano, Alaska: Quaternary Geochronology, v. 3, p. 56–67.

Schneider, D.J., Scott, C., Wood, J., and Hall, J., 2006, Nexrad weather radar observations of the 2006 Augustine volcanic eruption [abs.]: Eos (American Geophysical Union Transactions), v. 87, Fall meeting supp., abs. V51C-1686.

Scott, W.E., and McGimsey, R.G., 1994, Character, mass, distribution, and origin of tephra-fall deposits of the 1989–1990 eruption of Redoubt Volcano, south-central Alaska: Journal of Volcanology and Geothermal Research, v. 62, p. 251–272.

Vallance, J.W., Bull, K.F., and Coombs, M.L., 2010, Pyroclastic flows, lahars, and mixed avalanches generated during the 2006 eruption of Augustine Volcano, *in* Power, J.A., Coombs, M.L., and Freymueller, J.T., eds., The 2006 eruption of Augustine Volcano, Alaska: U.S. Geological Survey Professional Paper 1769 (this volume).

Venzke, E., Wunderman, R.W., McClelland, L., Simkin, T., Siebert, L., and Mayberry G., eds., 2002, Global Volcanism, 1968 to present: Smithsonian Institution, Global Volcanism Program Digital Information Series GVP-4 [http://www.volcano.si.edu/world/reports/, accessed on February 12, 2007].

Webley, P.W., Dean, K.G., Dehn, J., Bailey, J.E., and Peterson, R., 2010, Volcanic-ash dispersion modeling of the 2006 eruption of Augustine Volcano using the Puff model, *in* Power, J.A., Coombs, M.L., and Freymueller, J.T., eds., The 2006 eruption of Augustine Volcano, Alaska: U.S. Geological Survey Professional Paper 1769 (this volume).

Webster, J.D., Mandeville, C.W., Goldoff, B., Coombs, M.L., and Tappen, C., 2010, Augustine Volcano—The influence of volatile components in magmas erupted A.D. 2006 to 2,100 years before present, *in* Power, J.A., Coombs, M.L., and Freymueller, J.T., eds., The 2006 eruption of Augustine Volcano, Alaska: U.S. Geological Survey Professional Paper 1769 (this volume).

Appendix 1. Proximal Tephra Sample Station Locations on Augustine Island

Table 5. Proximal sample station locations on Augustine Island.

[All locations shown in datum WGS-1984; latitude and longitude are given in decimal degrees. The prefix "06AU" has been removed from all station names for brevity. PF, pyroclastic flow]

Station Name	Date Visited	Latitude	Longitude	Location Description
KLW020	7/31/2006	59.3857	-153.5154	NW Lagoon (south side west lands)
KLW021	7/31/2006	59.3872	-153.5156	NW Lagoon (south side west lands)
KLW022	7/31/2006	59.3867	-153.5190	NW Lagoon (south side west lands)
KLW023	8/1/2006	59.3683	-153.3670	1986 PF surface above Mound
KLW024	8/1/2006	59.3747	-153.3823	Northeast sector; south of seismic station AU14
KLW025	8/1/2006	59.3758	-153.3835	Feather edge of PF or lahar deposit
KLW026	8/1/2006	59.3718	-153.3929	Near ridge just below seismic station AU14
KLW027	8/1/2006	59.3469	-153.3810	Uphill of SE Point
KLW028	8/2/2006	59.3453	-153.4861	Reworked surge deposit in stressed alder
KLW029	8/2/2006	59.3382	-153.4591	Ridge south of Augustine Creek PF (tephra with abundant black dense juvenile clasts)
KLW030	8/2/2006	59.3367	-153.4565	Valley imediatly south of 06AUKW029
KLW031	8/2/2006	59.3358	-153.4173	Ridge south of AVO2/AV1
KLW032	8/2/2006	59.3244	-153.4147	South Point bluff
KLW033	8/2/2006	59.3484	-153.4797	Feather edge of SW PF finger (lower slopes);surges
KLW034	8/4/2006	59.3642	-153.3748	Near East Chute PF
KLW035	8/4/2006	59.3391	-153.3906	East Side
KLW036	8/4/2006	59.3999	-153.4494	Rocky Point PF
KLW037	8/4/2006	59.3628	-153.4446	Seismic station AUH
KLW038	8/4/2006	59.3284	-153.4006	SE coast near seal haul out (near South Point)
KLW039	8/5/2006	59.3786	-153.3475	NE Point Exactly
KLW040	8/5/2006	59.3569	-153.3420	East Point Bluff
KLW041	8/5/2006	59.3491	-153.3514	Between SE Point and S Point east of 2006 flowage deposits that enter the sea
KLW042	8/5/2006	59.3311	-153.4408	Between South Point and Augustine Creek PF
KLW043	8/5/2006	59.3221	-153.4947	Flats near West Lagoon
KLW044	8/5/2006	59.3471	-153.5305	West Lagoon
KLW045	8/5/2006	59.3835	-153.5509	West Island
KLW046	8/6/2006	59.3599	-153.4320	Summit-west
KLW047	8/6/2006	59.3596	-153.4285	Summit-east
KLW048	8/6/2006	59.3609	-153.4326	Summit-northwest side
KLW049	8/6/2006	59.3601	-153.4358	Ballistic field
KLW050	8/7/2006	59.3590	-153.4827	West side, upper alder stand
KLW051	8/7/2006	59.3594	-153.4840	West side transect
KLW052	8/7/2006	59.3600	-153.4856	West side transect
KLW053	8/7/2006	59.3608	-153.4865	West side transect
KLW054	8/7/2006	59.3615	-153.4869	West side transect
KLW055	8/7/2006	59.3616	-153.4869	West side transect
KLW056	8/7/2006	59.3618	-153.4870	West side transect
KLW057	8/7/2006	59.3702	-153.4879	West side transect

Table 5. Proximal sample station locations on Augustine Island.—Continued

[All locations shown in datum WGS-1984; latitude and longitude are given in decimal degrees. The prefix "06AU" has been removed from all station names for brevity. PF, pyroclastic flow]

Station Name	Date Visited	Latitude	Longitude	Location Description
KLW058	8/7/2006	59.3817	-153.4665	West side transect
KLW059	8/7/2006	59.3825	-153.4672	West side transect
KLW060	8/7/2006	59.3850	-153.4681	West side transect
KLW061	8/7/2006	59.3857	-153.4676	West side transect
KLW062	8/7/2006	59.3865	-153.4671	West side transect
KLW063	8/7/2006	59.3907	-153.4734	West side transect
KLW064	8/8/2006	59.3929	-153.4442	East side of ridge above Rocky Point PF
KLW065	8/8/2006	59.3935	-153.4449	West side of ridge above Rocky Point PF
KLW066	8/8/2006	59.3944	-153.4452	Ridge above Rocky Point PF, near surge
KLW067	8/8/2006	59.3955	-153.4457	Surge deposit western side of Rocky Point PF
KLW068	8/8/2006	59.3955	-153.4454	Surge deposit western side of Rocky Point PF
KLW069	8/8/2006	59.4040	-153.4467	Edge of Rocky Point PF, coastwise
KLW070	8/8/2006	59.4072	-153.4434	Just north of Rocky Point in hummocky topography
KLW071	8/8/2006	59.4081	-153.4438	Coastward of KW070 just north of Rocky Point
KLW072	8/8/2006	59.4077	-153.3949	Burr Point vicinity
KLW073	8/8/2006	59.4065	-153.3988	Burr Point vicinity
KLW074	8/8/2006	59.3858	-153.3818	North of NE Point where larger of 2006 lahars nears the coast
KLW075	8/9/2006	59.3405	-153.3991	East side near seismic station AUSE
KLW076	8/9/2006	59.3584	-153.3709	Upper Alder between East Point and SE Point, lahar visible to north
KLW077	8/9/2006	59.3584	-153.3719	Very near 06AUKW076
KLW078	8/9/2006	59.3642	-153.3751	East side; in high alder
KLW079	8/9/2006	59.3780	-153.4766	NW sector, west of Windy PF; in willow
KLW080	8/9/2006	59.3792	-159.4799	NW sector, west of Windy PF; in alder
KLW081	8/9/2006	59.3577	-153.5259	West sector, in low alder
KLW082	8/10/2006	59.3773	-153.5193	AVO field camp location
KW083	8/10/2006	59.3702	-153.3538	Benchmark Mound
KW084	9/25/2006	59.3254	-153.4667	SSW coast
KW085	9/25/2006	59.3248	-153.4667	SSW coastal bluff (prehistoric Augustine tephra fall)
TP001	12/20/2005	59.3486	-153.4216	Lower south flank
MC001	1/12/2006	59.3694	-153.4730	West flank of Augustine. Ash collection site AAW (seismic station AUW)
MC002	1/12/2006	59.4118	-153.4161	Burr Point. Ash collection site AAN

Appendix 2. Raw Electron Microprobe Geochemical Analyses of Glass from Augustine 2005–2006 Tephra

[This appendix appears only in the digital version of this work—in the DVD-ROM that accompanies the printed volume and as a separate file accompanying this chapter on the Web at: http://pubs.usgs.gov/pp/1769]

Table 6 is a Microsoft Excel file that contains the data used to derive table 2 and figure 7 after analyses were filtered to eliminate the inclusion of mineral data and other bad data points.